Biosynthetic Routes to Short-Chain Carboxylic Acids and Their Hydroxy Derivatives

A Thesis

SUBMITTED TO THE FACULTY OF

UNIVERSITY OF MINNESOTA

BY

Yogesh K. Dhande

IN PARTIAL FULFILLMENT OF THE REQUIREMENTS
FOR THE DEGREE OF

MASTER OF SCIENCE

Adviser: Prof. Kechun Zhang

July 2013

Abstract

The current drive for sustainable routes to industrial chemicals and energy due to depleting fossil reserves has motivated research in the field of biotechnology. Biomass is abundant on earth and photosynthesis, if utilized properly, can lead the way to a sustainable carbon cycle. The recent advances in metabolic engineering, DNA sequencing, and protein engineering are driving research to achieve this goal. In this work, the native leucine and isoleucine biosynthetic pathways in *Escherichia coli* were expanded for the synthesis of pentanoic acid (PA) and 2-methylbutyric acid (2MB) respectively. Several aldehyde dehydrogenases and 2-ketoacid decarboxylases were studied for the conversion of ketoacids into respective carboxylic acids. The optimal combinations of these enzymes enabled production of 2.6 g/L 2MB with IPDC-AldH and 2.6 g/L of PA with IPDC-KDH_{ba} in shake-flask fermentations. The extension of these pathways to synthesize value-added chemicals like hydroxyacids was attempted. The cytochrome P450 BM-3 enzyme was engineered to enhance its ability to oxidize unactivated C-H bonds in the short-chain carboxylic acids. Nine mutants were created by rational. The mutant L437K showed 20 to 30-fold higher activity compared to the wild-type. A screening strategy was developed to evolve isobutyrate-hydroxylating activity in P450s based on the valine degradation pathway in *Pseudomonas aeruginosa*. As a growth-based selection strategy, it will allow screening of a large library. This work expands the library of chemicals that can be produced biologically as a step forward to the sustainable future.

Contents

List of Tables

List of Figures

Chapter 1

Introduction

Nature has developed a vast array of capabilities through years of evolution that are being rapidly discovered and incorporated into useful constructions. Advances in molecular biology, macromolecular crystallography, and DNA sequencing are making possible a rapid characterization of biological parts. This has facilitated the recent boom in metabolic and protein engineering efforts. This work presents two such efforts aimed at development of new biosynthetic pathways for short-chain monocarboxylic acids and their hydroxy derivatives.

Organization and summary

This chapter provides a general motivation for the development of new biosynthetic pathways and enzyme functions. The background establishes the importance and current status of biosynthetic approaches. Short-chain carboxylic acids and their hydroxy derivatives are discussed for their practical importance. Natural environments where they are observed and the need for engineered pathways are discussed. Furthermore, the chapter introduces amino acid biosynthetic pathways as important metabolic channels for development of synthetic pathways. Cytochrome P450 enzymes are introduced at the end of the chapter as catalysts capable of oxidizing unactivated C-H bonds.

Chapter 2 begins with the description of synthetic metabolic pathways for pentanoic acid and 2-methylbutyrate. The incorporation of two nonnatural steps, the decarboxylation of ketoacids and their oxidation to carboxylic acids, are discussed in detail. Active enzymes

are identified for each of these steps in the two pathways and their activities are characterized in vitro. This chapter describes the shake-flask production and time-course experiments to quantify the metabolite production rates and yields.

Chapter 3 discusses literature on P450 catalyzed hydroxylation of carboxylic acids relevant to this work and an attempt at rational engineering of the P450 binding site. This rational approach was guided by previous research, computational analysis of the P450-substrate binding conformation, and visualization of the crystal structure with PyMOL. Nine mutants were created and studied for their activities on five and six-carbon carboxylic acid substrates. For comparison, wild-type P450 and one published mutant were also included in the study. The results of these cell extract experiments were verified by purifying and characterizing the mutant L437K which exhibited the highest activity along with the L181K mutant described in the literature and wild-type enzyme.

Chapter 4 provides a brief summary of the work and presents conclusions drawn from the experiments described in chapters 2 and 3. It also outlines directions for future work. Finally, chapter 5 describes the experimental procedures used for the studies discussed in this thesis. A section on supplementary data is included at the end to present data that is important to this work but was excluded in earlier chapters to achieve conciseness.

Motivation and background

Crude oil has been a major source of energy and chemicals for our society from the last century. However, these reserves are being actively depleted resulting in increased oil prices (prices have more than doubled in last 20 years) [1, 2]. This has necessitated the development of sustainable routes to fuels and chemicals. Much effort has been devoted

to research in renewable biofuels such as alcohols, biodiesel and alkanes. Solar, wind, and geothermal sources of energy are also being considered as renewable, safe and potentially environment-friendly alternatives to fossil fuels; however, these technologies cannot provide replacement for the various chemicals used in industry and our daily lives. For this reason, there is also an urgent need to establish sustainable routes to these widely used chemicals. This work aims to provide such sustainable routes to carboxylic acids and their hydroxy derivatives, which are important chemical intermediates.

Lignocellulosic biomass is the most abundant renewable source of carbon. According to a recent report by the Department of Energy, the United States has the potential to produce 1.3 billion tons of it annually [3]. Cellulose composes a significant fraction of this biomass [4]. It is a polymer composed of a linear chain of glucose molecules. Glucose, being biologically derived, is more suitable for selective conversions by biological rather than traditional chemical processes [5]. Biosynthesis also offers several other advantages over the traditional chemical methods. It is typically safe and environmentally friendly as it is employed under mild conditions and in absence of toxic chemicals. Whole cells can act as catalysts capable of promoting several reactions that can covert a common feed material like glucose into complex structures. This is of great importance since it allows one-pot synthesis of desired chemicals.

Substantial interest exists to explore biosynthesis to tap into the renewable biomass-based resources for a sustainable supply of chemicals and energy [6-8]. The biomass-based sustainable cycle is envisioned which comprises of growing cellulosic biomass, deconstruction of cellulose into glucose, biotransformation of glucose into useful

chemicals or fuels, and their transport and use. There are several challenges associated with each of the steps in the cycle and significant efforts are being made to address them [6, 7, 9]. The present work fits into the penultimate step in this cycle: biotransformation of glucose into useful chemicals.

Despite the many advantages of biosynthesis, many challenges exist [10] in its application for development of a sustainable chemical industry. The number of chemicals produced via biosynthesis is still very small despite the potential for diversity that it offers. This work aims to expand this repertoire of chemicals by introducing biosynthetic pathways to short chain carboxylic acids and their hydroxy derivatives. Other challenges include low yields and concentrations, large reactor volumes, and difficult separation processes. These will not be the topics of discussion in this work, but are important considerations for future development of the results presented in chapters 2 and 3.

Production of nonnatural metabolites requires development of synthetic metabolic pathways. The recent advances in the field of biotechnology have facilitated the rapid development of such approaches. Some of these enabling technologies relevant to this work are heterologous protein expression [11], metabolic engineering [12], DNA sequencing [13], and protein engineering [14, 15]. The next three paragraphs will establish the importance of these technologies and their relevance to this work.

Metabolic engineering has emerged as a promising tool for enhancing the biosynthesis of a wide variety of chemicals in host organisms. It aims at enabling and optimizing the production of desired chemicals by tweaking the metabolism of a host organism. This is achieved by adding or removing reactions from the metabolic network as well as tuning

the reaction rates and regulatory controls. Several examples already exist in which metabolic engineering has given economically viable production routes from glucose to high volume industrial chemicals such as ethanol [16], lactic acid [17] and citric acid [18]. At present, the number of chemicals produced in substantial quantities through biosynthesis is limited and many of these processes are not economical due to low concentrations in the product stream and associated high costs of recovery. Therefore, it has become imperative to develop biological strains and processes capable of producing high yields of nonnatural chemicals relevant to the chemical industry. Some examples of such chemicals for which biosynthetic pathways have been engineered are 1,3-propanediol [19], isobutanol [20], homoalanine [21] and 1,4-butanediol [22]. Such nonnatural pathways often utilize the property exhibited by many enzymes known as "promiscuity", which means that the enzyme shows activity on other substrates, often belonging to a particular class, in addition to their natural substrate [23, 24]. Even though the activity on such substrates is usually lower, such promiscuity provides a framework for engineering nonnatural metabolic pathways.

Advances in DNA sequencing have truly accelerated the growth of biotechnology. The reduced prices and turnover times are allowing rapid sequencing of new organisms. This has greatly facilitated the identification and cloning of genes for metabolic engineering applications. Chapter 2 will describe the search and cloning of genes enabled by such sequencing data.

Protein engineering is critical to enable reactions that are not found in nature. The goal of protein engineering is to alter the enzyme structure to allow nonnatural reactions or

enhance the existing reaction. Two approaches, rational design and directed evolution, are widely employed to achieve these goals. Chapter 3 will describe the use of both these approaches to allow hydroxylation of short-chain carboxylic acids.

Short-chain carboxylic acids

Natural organisms have been found to produce C2-C4 acids such as acetic acid [25], propionic acid [26] and butyric acid [27]. However, there are very few reports [28-30] of single organisms capable of producing significant quantities of higher monocarboxylic acids like pentanoic acid (PA) (also known as valeric acid) and 2-methylbutyric acid (2MB) directly from glucose without supplementing additional chemicals. The total U.S. consumption of PA and 2MB was approximately 14,000 metric tons in 2005 [31]. These chemicals serve as intermediates for a variety of applications such as plasticizers, lubricants and pharmaceuticals. They are also used for extraction of mercaptans from hydrocarbons. Esters of valeric acid as valeric biofuels are also gaining increased attention, as they can be used in both gasoline and diesel with very high blend ratios [32]. Commercially, these chemicals are manufactured by the oxo process in which 1-butene and 2-butene react with synthesis gas (a mixture of carbon monoxide and hydrogen) to make valeraldehyde and 2-methylbutyraldehyde followed by their oxidation to respective acids [31]. Since the process uses toxic intermediates like synthesis gas and non-renewable petroleum-based feedstock, a sustainable route to these chemicals is needed. Biosynthesis can provide a potential alternative route to these chemicals.

2MB and PA have been observed in nature as the products of anaerobic metabolism. 2MB has been reported as the major product (about 20%) of anaerobic metabolism of

parasitic intestinal helminths such as *Ascaris lumbricoides* and *Ascaris suum* [33, 34]. Propionate and acetate produced from either glucose or lactate serve as the precursors for the synthesis of 2MB in these organisms [34]. There have also been reports of valerate accumulation during metabolism of mixed rumen microorganisms [35, 36] as well as during the production of hydrogen by a mixed culture of fermentative bacteria [37]. However the C5 acids are produced in the byproduct pathways that have not been optimized for their production and the reported quantities of both these compounds are very small. In this work, biosynthetic strategies were developed for the renewable production of pentanoic acid and 2-methylbutyric acid from glucose. To achieve this goal, the amino acid biosynthetic pathways were explored for the production of these compounds.

The amino acid biosynthetic pathways have been successfully utilized for the production of alcohols [20, 38, 39] and carboxylic acids [40, 41]. These pathways generate a variety of ketoacids that can potentially be converted into many useful products. Moreover, since these pathways exist in every organism, a wide range of host organisms can be explored once the proof of concept is achieved. In case of the alcohol production using these pathways, the ketoacids were decarboxylated to aldehydes, which were reduced by alcohol dehydrogenase enzyme to alcohols. These aldehydes can, in principle, be oxidized to corresponding carboxylic acids. The challenge is to identify enzymes capable of carrying out this conversion. Chapter 2 describes this search for the active enzymes and provides a proof-of-concept for biosynthesis of these acids via shake-flask production experiments.

Hydroxy derivatives of short-chain carboxylic acids

In addition to valerate and 2-methylbutyrate, biosynthesis of other acids such as isobutyrate, 3-methylbutyrate and 4-methylvalerate has been demonstrated in our lab previously [40, 41]. These acids are important intermediates for the chemical industry with applications in making a wide variety of chemicals. One such application is the production of hydroxyacids. Hydroxyacids are high value chemicals with applications in nutritional supplements and cosmetics [42]. They are chiral molecules and serve as important chiral synthetic building blocks for amino acids, peptides and antibiotics. Hydroxyacids are also attractive monomers because their polymers are typically degradable [43] and biocompatible [44]. However, not many are used for making polymers due to the high costs of production. Hydroxyacids are difficult to synthesize by traditional chemical methods because of their low selectivity and the downstream expensive separation processes required. As a result, the sustainable polymers market is currently dominated only by polylactic acid, which is made from biologically produced lactic acid. However, polylactic acid has some disadvantages: low resistance to heat and humidity, low flexibility and low mold cycle time. A larger repertoire of hydroxyacids can provide polymers with diverse physical and mechanical properties. Biosynthesis of such monomers from glucose has the potential to provide a sustainable route to these high volume materials thus reducing the reliance on petroleum and its impact on the environment.

Another hydroxyacid of interest is L-3-hydroxyisobutyrate (HIBA). The production of such chiral compound becomes very expensive because it requires resolution of racemic mixtures and recovery and recycle of expensive resolving agents. HIBA is used as an

intermediate in tocopherol synthesis. It can also be potentially used as a monomer to produce biodegradable poly(hydroxyisobutyrate) polymer. Alternatively, it can be dehydrated to produce methacrylate which can then be used to make polymethacrylate (PMA) or poly(methyl methacrylate) (PMMA). U.S. methyl methacrylate production capacity is approximately 2.2 million tons per year used predominantly for making PMMA which is used as an alternative to glass or polycarbonate in optical instruments, medical devices and household accessories. Chapter 3 describes a novel growth-based screening strategy for discovery of isobutyrate-hydroxylating enzymes.

Long chain carboxylic acids are known to be hydroxylated by cytochrome P450 enzymes. Cytochrome P450s belong to a broad class of external monooxygenases and are ubiquitous in nature [45, 46]. Cytochrome P450 BM-3 from *Bacillus megaterium* [47] is one of the most widely studied P450. It has many properties that make it attractive for biotechnological applications [48-50]. Unlike many other P450s, P450 BM-3 is soluble which allows for easy expression in a model organism such as *E. coli* and characterization. Also the reductase domain is fused to the catalytic domain that contains the hemoprotein [51]. The reductase domain derives two electrons from one molecule of NADPH and transfers it to the catalytic domain [52]. These electrons are used to reduce molecular oxygen [53]. One atom of oxygen is incorporated into the substrate while the other gets reduced to water.

P450 BM-3 has been widely studied and is shown to be promiscuous in oxidizing a wide range of substrates. It has been engineered to have activity on alkanes such as octane [54] and propane [55, 56], aromatic hydrocarbons naphthalene [57], and alkenes like styrene

[58]. One such study relevant to this work was engineering of P450 to extend the substrate range to smaller carboxylic acids [59]. The native substrates studied for P450 enzymes include C12 to C18 acids [60]. Ost et al. (2000) rationally engineered the active site of P450 and showed improved activities on C4 to C8 substrates. Even though the reported activities are not high enough to drive their use in metabolic engineering, it provides an attractive framework for biosynthesis of short-chain hydroxyacids. Chapter 3 will describe an effort to engineer P450 BM-3 for hydroxylation of short-chain chain acids with the goal of using it in the metabolic production of hydroxyacids.

An important limitation in biological production of chemicals is that the products are present in very low concentration which makes their separation and purification economically unfavorable [61]. Also, lowering of pH due to production of acids affects cell growth negatively [62]. Both these limitations can be avoided by polymerizing the hydroxyacids as soon as they are produced. Polyhydroxyalkanoates (PHAs) production using microorganisms has gained a lot of attention recently [63, 64]. The pathways developed in this work will expand the scope of PHAs beyond naturally occurring monomers.

Chapter 2

Production of C5 Carboxylic Acids

As discussed in chapter 1, in addition to fuels, there is also an urgent need to establish sustainable routes to commonly used industrial chemicals. The aim of this study was to demonstrate the construction of engineered *E. coli* strains capable of producing C5 carboxylic acids.

Construction of synthetic metabolic pathways

The amino acid biosynthetic pathways introduced in chapter 1 were investigated for the production of the target C5 compounds. The native leucine and isoleucine biosynthetic pathways in *E. coli* were expanded by the introduction of aldehyde dehydrogenases and 2-ketoacid decarboxylases. The synthetic metabolic routes to 2MB and PA from glucose are given in Figure 1. A common intermediate for both the pathways is 2-ketobutyrate (2KB), which is derived from threonine by biosynthetic deaminase IlvA. Overexpressing thrA, thrB, and thrC drives the carbon flux towards threonine biosynthesis [8].

For the synthesis of 2MB, 2KB is driven into synthesis of 2-keto-3-methylvalerate (KMV), the penultimate precursor to 2MB. The condensation of 2KB and pyruvate to 2-aceto-2-hydroxybutyrate (AHB) is catalyzed by IlvG and IlvM. Another two enzymes, IlvC and IlvD, are required to catalyze the conversion of AHB to KMV. KMV is then decarboxylated by a ketoacid decarboxylase (DC) into 2-methylbutyraldehade, which is oxidized to 2MB by an aldehyde dehydrogenase (DH).

For the synthesis of PA, 2KB needs to go through two cycles of "+1" carbon chain elongation [65] to make 2-ketocaproate (2KC). In leucine biosynthetic pathway, 2-ketoisovalerate is converted to 2-ketoisocaproate through a 3-step chain elongation cycle catalyzed by 2-isopropylmalate synthase (LeuA), isopropyl malate isomerase complex (LeuC, LeuD) and 3-isopropylmalate dehydrogenase (LeuB). It was previously demonstrated that LeuA, LeuB, LeuC, and LeuD are promiscuous enough to allow 2KB to go through the same elongation cycle to produce 2-ketovalerate (2KV) and further to 2-ketocaproate (2KC) (4). 2KC is then decarboxylated by a DC into valeraldehyde and oxidized subsequently to PA by a DH.

All the enzymes downstream of aspartate biosynthesis were overexpressed from three synthetic operons. The constructed operons for PA and 2MB are shown in Figure 2. The genes thrA, thrB and thrC involved in threonine synthesis were present in the first operon under the regulation of $P_L$lacO1 promoter on a low-copy plasmid carrying a spectinomycin resistance marker. For 2MB synthesis, ilvA, ilvG, ilvM, ilvC, and ilvD were cloned on a medium-copy plasmid with a kanamycin resistance marker. For the synthesis of PA, ilvA, leuA, leuB, leuC and leuD were cloned on a medium-copy plasmid carrying a kanamycin resistance marker. Various aldehyde dehydrogenases and ketoacid decarboxylases were present in the transcriptional order DC-DH on high copy plasmids carrying an ampicillin resistance marker.

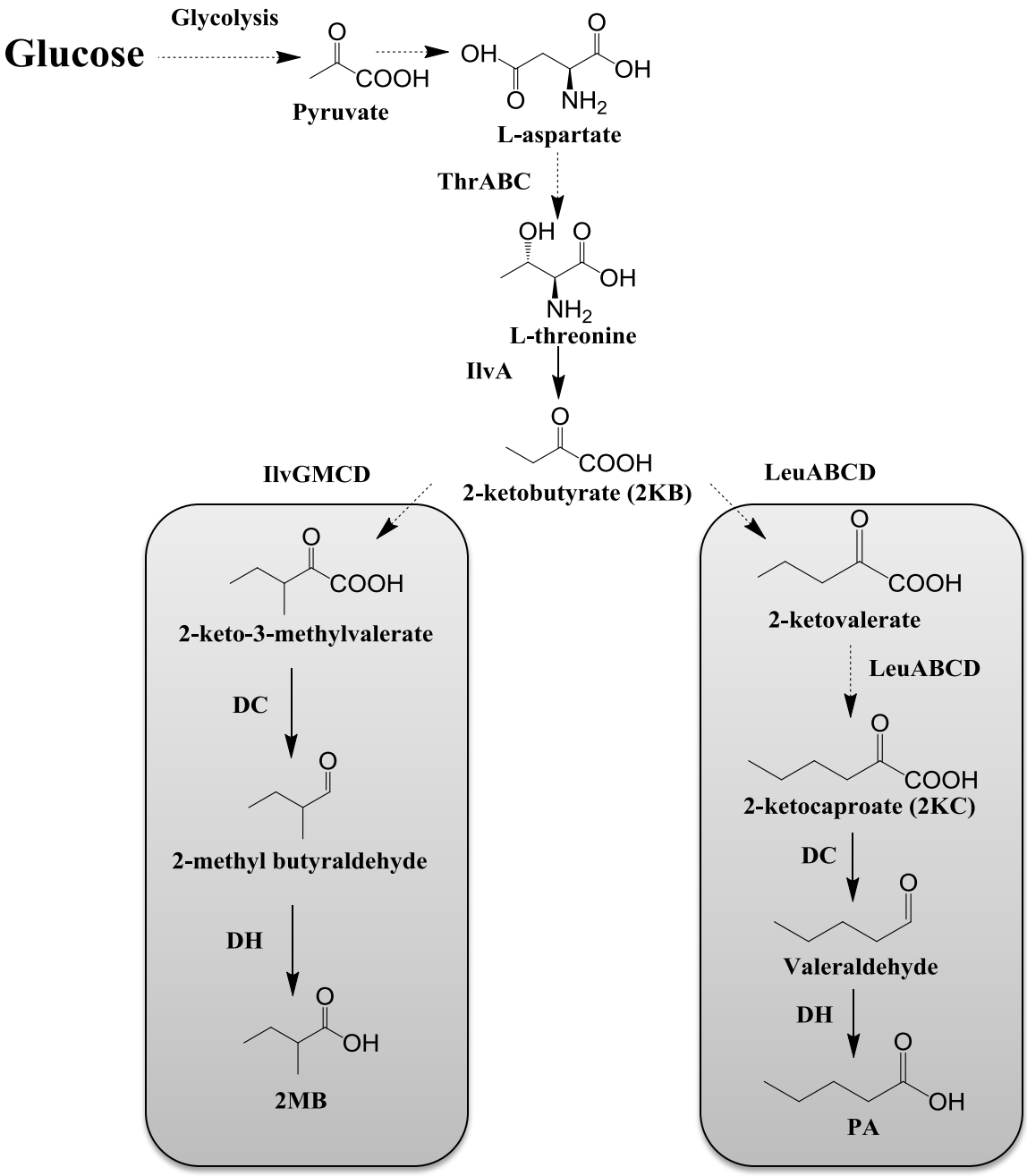

Figure 1: Synthetic metabolic pathways for the production of 2-methylbutyric acid (2MB) and pentanoic acid (PA). Nonnatural metabolic steps are shaded. DC, 2-ketoacid decarboxylase; DH, aldehyde dehydrogenase. Dotted arrows indicate that multiple steps are involved.

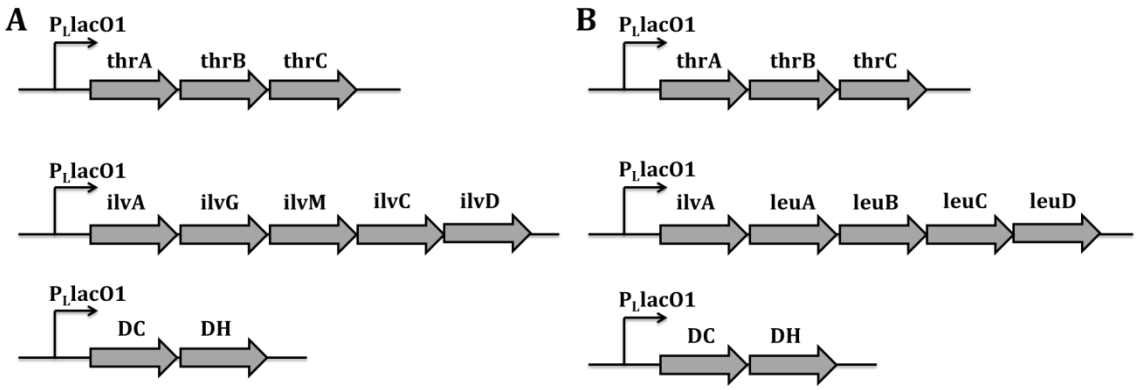

Figure 2: Synthetic operons for (A) 2-methylbutyric acid (2MB) production, (B) pentanoic acid (PA) production. DC, 2-ketoacid decarboxylase; DH, aldehyde dehydrogenase.

Since threonine is a common intermediate in both the pathways, a threonine overproducer *E. coli* strain ATCC98082 was used in the study. The strain had threonine exporter gene rhtA knocked out to ensure high intracellular levels of threonine [21]. The alcohol dehydrogenase yqhD gene deletion was performed to eliminate the side reactions leading to production of alcohols [40]. The resultant strain is referred to hereafter as the PA1 strain. The various strains and plasmids used in this study are listed in table 1.

Table 1: Strains and plasmids used in the study

Strains	**Description**	**Reference/source**
PA1	ATCC98082(ΔrhtA, ΔyqhD)	This study
XL10-Gold	Tet^{r}Δ (*mcrA*)*183* Δ (*mcrCB-hsdSMR-mrr*)*173 endA1 supE44 thi-1 recA1 gyrA96 relA1 lac* Hte [F´ *proAB lacI*^{q}Z*DM15* Tn*10* (Tet^r) Amy Cam^r]	Stratagene
XL1- Blue	*recA1 endA1 gyrA96 thi-1 hsdR17 supE44 relA1 lac* [F´ *proAB lacI*^{q}Z*ΔM15* Tn*10* (Tet^r)]	Stratagene
Plasmids	**Description**	**Reference/source**
pIPA1	psc101 ori; Spec^r; $P_L$lacO1: thrA-thrB-thrC	[39]
pIPA2	p15A ori; Kan^r; $P_L$lacO1: ilvA-ilvG-ilvM-ilvC-ilvD	This study
pIPA3	p15A ori; Kan^r; $P_L$lacO1: ilvA-leuA-leuB-leuC-leuD	This study
pIPA4	ColE1 ori; Amp^r; $P_L$lacO1: kivD-padA	[40]
pIPA5	ColE1 ori; Amp^r; $P_L$lacO1: kivD-aldB	[40]
pIPA6	ColE1 ori; Amp^r; $P_L$lacO1: kivD-gabD	[40]
pIPA7	ColE1 ori; Amp^r; $P_L$lacO1: kivD-KDH_{ba}	[40]
pIPA8	ColE1 ori; Amp^r; $P_L$lacO1: kivD-aldH	[40]
pIPA9	ColE1 ori; Amp^r; $P_L$lacO1: kivD-ydcW	[40]
pIPA10	ColE1 ori; Amp^r; $P_L$lacO1: kivD V461A/F381L-padA	[41]
pIPA11	ColE1 ori; Amp^r; $P_L$lacO1: kivD V461A/F542L-padA	[41]
pIPA12	ColE1 ori; Amp^r; $P_L$lacO1: kivD V461A/M538A-padA	[41]
pIPA13	ColE1 ori; Amp^r; $P_L$lacO1: IPDC-padA	[41]
pIPA14	ColE1 ori; Amp^r; $P_L$lacO1: IPDC-aldH	This study
pIPA15	ColE1 ori; Amp^r; $P_L$lacO1: IPDC-KDH_{ba}	[41]
pIPA16	ColE1 ori; Amp^r; $P_L$lacO1: 6xhis-aldH	This study

Synthesis of C5 carboxylic acids

The key steps in the designed pathways are decarboxylation of ketoacids KMV and 2KC into respective aldehydes, followed by oxidation to carboxylic acids. The success of this strategy was dependent on the discovery of enzymes that can catalyze these reactions. Based on our previous work on producing isobutyric acid [40], wild-type 2-ketoisovalerate decarboxylase KIVD from *Lactococcus lactis* [66] and phenylacetaldehyde dehydrogenase PadA [67] from *E. coli* were cloned on a high-copy plasmid pIPA4 to check for the production of target chemicals. KIVD has been previously shown to have a wide substrate range for converting 2-ketoacids into aldehydes [38, 39]. The PA1 strain was transformed with plasmids pIPA1, pIPA2 and pIPA4 for 2MB and plasmids pIPA1, pIPA3 and pIPA4 for PA synthesis. Shake-flask experiments were carried out with the recombinant strain at 30 °C and samples were analyzed by HPLC as described in Chapter 5. Through this, productions titers of 2.3 g/L for 2MB and 2.1 g/L for PA were achieved which demonstrated the feasibility of our biosynthetic approach.

Screening of aldehyde dehydrogenases

In order to improve production titers, several aldehyde dehydrogenases were studied for their activity in the pathway (Figure 3). It was speculated that some of the aldehyde dehydrogenases found in nature will be promiscuous enough to catalyze these conversions. Six such enzymes (including PadA) were selected as candidate enzymes for this study. These were acetaldehyde dehydrogenase AldB [68], 3-hydroxypropionaldehyde dehydrogenase AldH [69], phenylacetaldehyde dehydrogenase

PadA [67], succinate semialdehyde dehydrogenase GabD [70], γ-aminobutyraldehyde dehydrogenase YdcW [71] from *E. coli*, and α-ketoglutaric semialdehyde dehydrogenase KDH_{ba} [72] from *Burkholderia ambifaria*. Strains were constructed with three synthetic operons as shown in Figure 2. All other enzymes except DHs were the same and wild-type KIVD was present as the DC for each strain. Shake-flask production experiments were carried out as described in Chapter 5. Since all the other enzymes were the same, the strain producing the highest quantity of desired product was assumed to have the most desirable aldehyde dehydrogenase.

To compare activities of various DHs in production of 2MB, the PA1 strain was transformed with plasmids pIPA1, pIPA2 and any one of pIPA4 to pIPA9. The highest titer of 2.5 g/L was achieved with AldH while AldB, PadA, KDH_{ba}, GabD and YdcW produced 2.3 g/L, 2.3 g/L, 0.67 g/L, 0.14 g/L and 0.23 g/L respectively. For production of PA, the PA1 strain was transformed with plasmids pIPA1, pIPA3 and any one of pIPA4 to pIPA9. KDH_{ba} was found to be most active aldehyde dehydrogenase for the production of PA (2.3 g/L), while AldH, AldB, PadA, GabD and YdcW produced 1.8 g/L, 0.42 g/L, 2.1 g/L, 0.54 g/L, and 0.22 g/L respectively. This indicated that AldH had the highest activity to synthesize 2MB but not significantly greater than PadA ($p=0.4$) and AldB ($p=0.07$). Similarly, KDH_{ba} had highest activity to synthesize PA but not significantly greater than PadA ($p=0.08$).

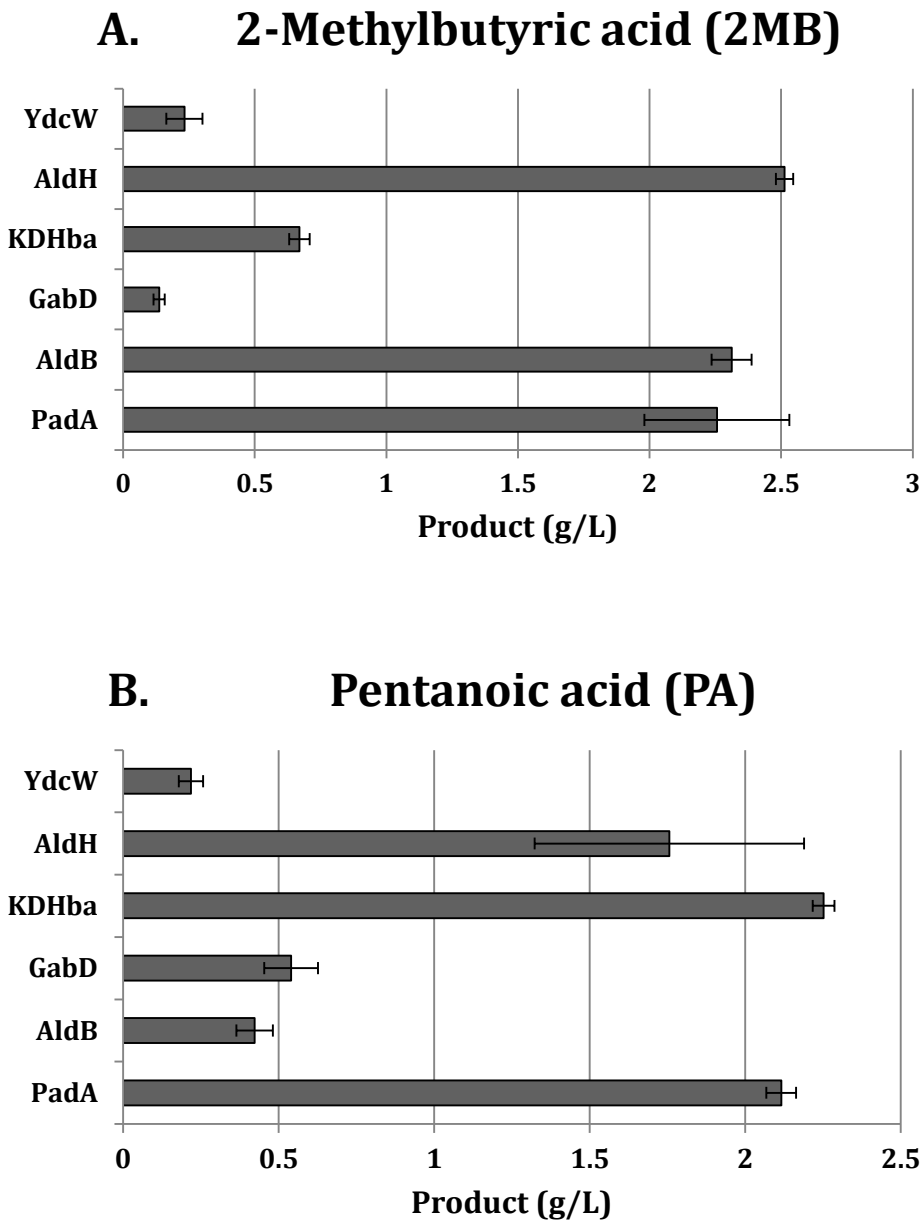

Figure 3: Results of production experiments with different aldehyde dehydrogenases. (A) Comparison of aldehyde dehydrogenases for 2MB production. (B) Comparison of aldehyde dehydrogenases for production of PA.

Screening of 2-ketoacid decarboxylases

Several byproducts such as acetate and isobutyrate during production of 2MB and acetate, butyrate and 3-methylbutyrate during production of PA were observed. Production of the C4 and C5 carboxylic acids is attributed to the broad range of substrate specificity exhibited by selected DCs and DHs. Rational engineering of KIVD to increase the substrate specificity has been published [39]. Mutation V461A was reported to increase the specificity of KIVD towards larger substrates. Effect of three more mutations M538A, F381L and F542L was investigated on top of V461A mutation. These mutations replace a bulky residue in key locations by a smaller hydrophobic residue and thus were expected to further increase the activity towards larger substrates.

Wild-type KIVD and its mutants were investigated for an increase in yield of target C5 acids and reduction in byproduct formation. The effect of indolepyruvate decarboxylase IPDC from *Salmonella typhimurium* (*S. typhi*) was also studied. *E. coli* and *S. typhi* share a common ancestor and so this protein was expected to express well in *E. coli* [73]. Similar to the earlier screening strategy, plasmids were constructed with different DCs but the same DH (PadA) and other enzymes.

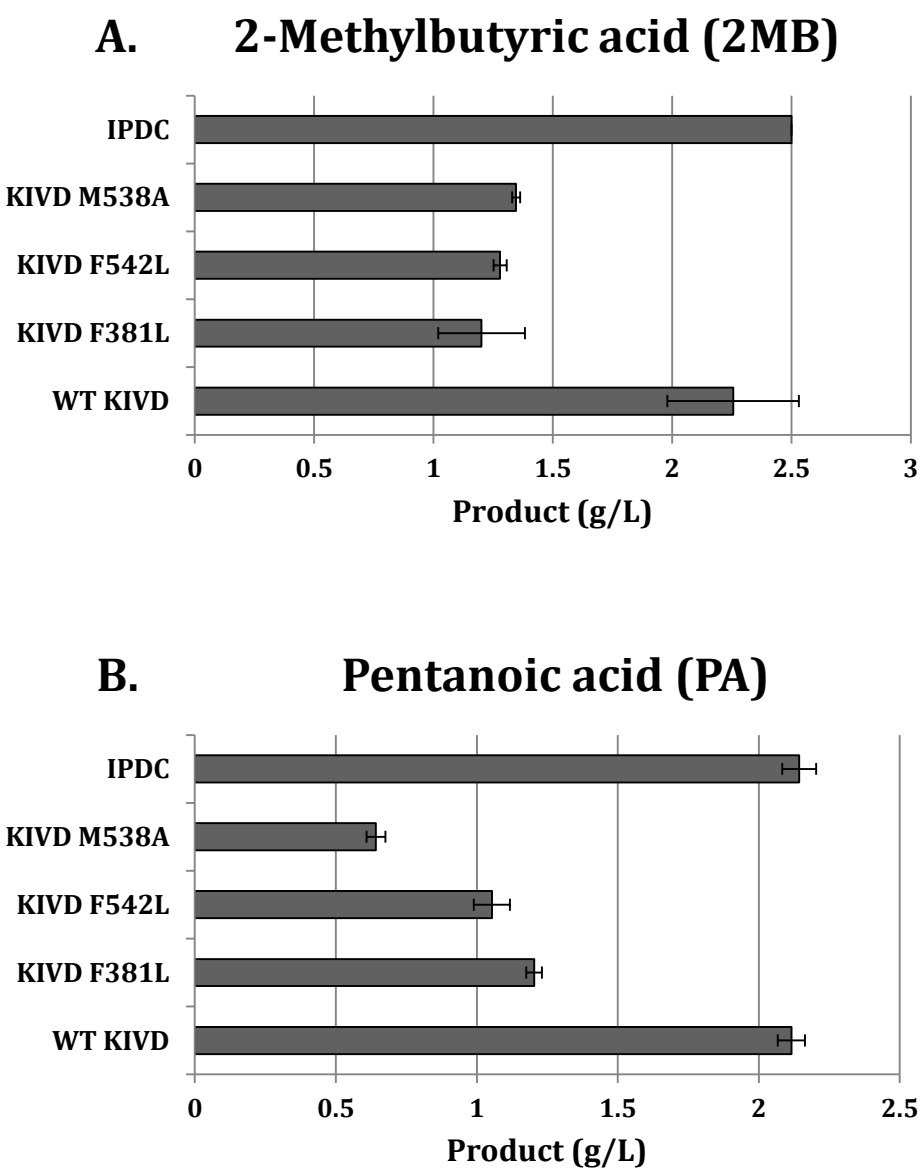

Figure 4: Results of production experiments with different ketoacid decarboxylases. (A) Comparison of ketoacid decarboxylases for 2MB production. (B) Comparison of ketoacid decarboxylases for production of PA.

To compare the activities of the selected DCs, the PA1 strain was transformed with pIPA1, pIPA2 and any one of the plasmids pIPA10 to pIPA13 for 2MB and pIPA1, pIPA3 and any one of the plasmids pIPA10 to pIPA13 for PA synthesis. Shake flask experiments showed higher production with IPDC than KIVD mutants for the production of both 2MB (2.5 g/L) and PA (2.1 g/L). However, the results were not statistically different than KIVD. Figure 4 shows the production results.

Production profiles of final strains

After having established that AldH and IPDC have the highest activity among all of candidate DHs and DCs for the production of 2MB, they were combined together (pIPA14) to investigate if the effects are additive. With their combination, 2MB titer achieved was 2.6 g/L. In comparison, the production titer was 2.5 g/L for AldH with WT KIVD and 2.5 g/L for PadA with IPDC (Figure 5A). Similarly, KDH_{ba} was cloned together with IPDC (pIPA15) for the production of PA. This increased PA titer to 2.6 g/L, higher than 2.3 g/L for KDH_{ba} with WT KIVD and 2.1 g/L for PadA with IPDC (Figure 5B).

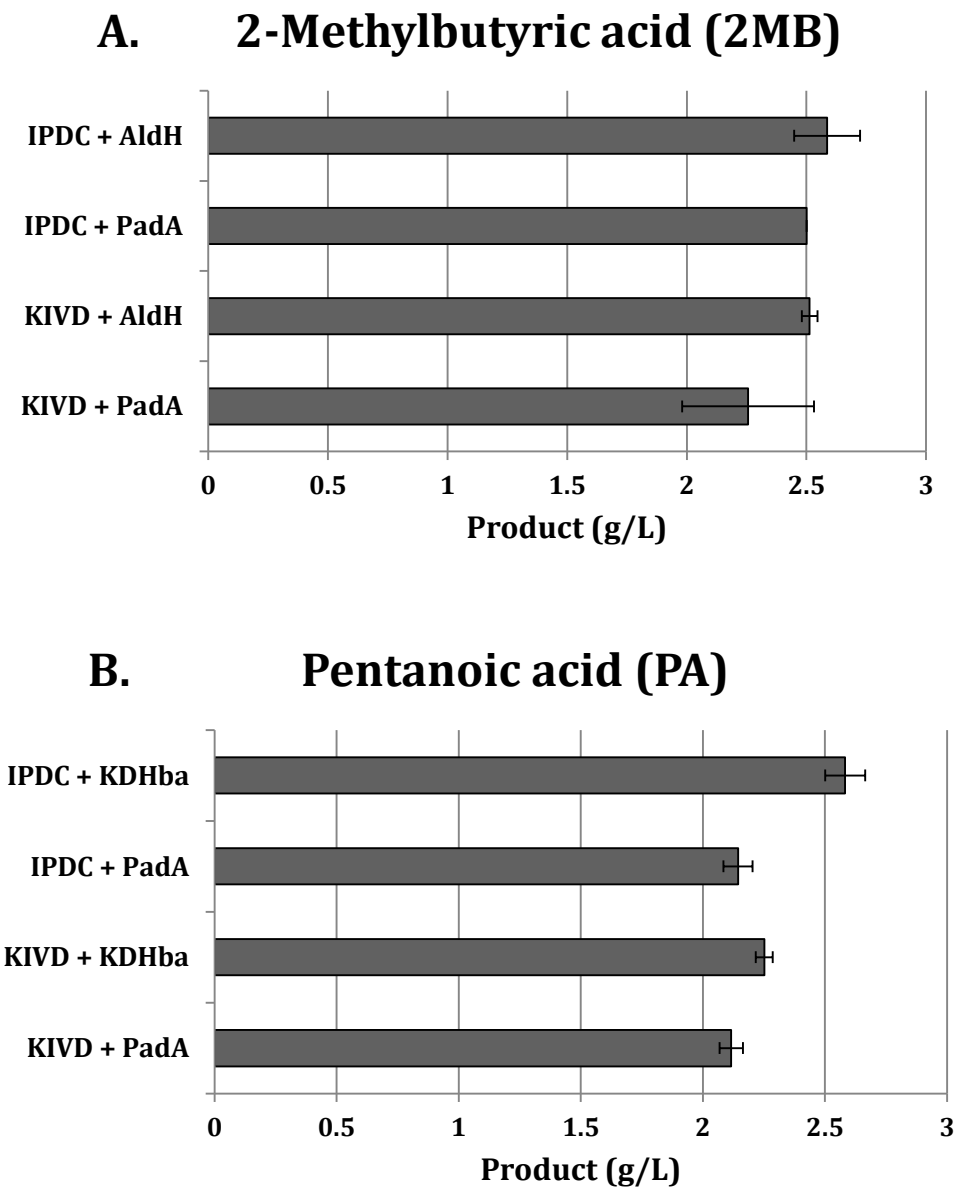

Figure 5: Results of production experiments for combinations of best ketoacid decarboxylases and aldehyde dehydrogenases. (A) Comparison of various combinations for 2MB production. (B) Comparison of various combinations for production of PA.

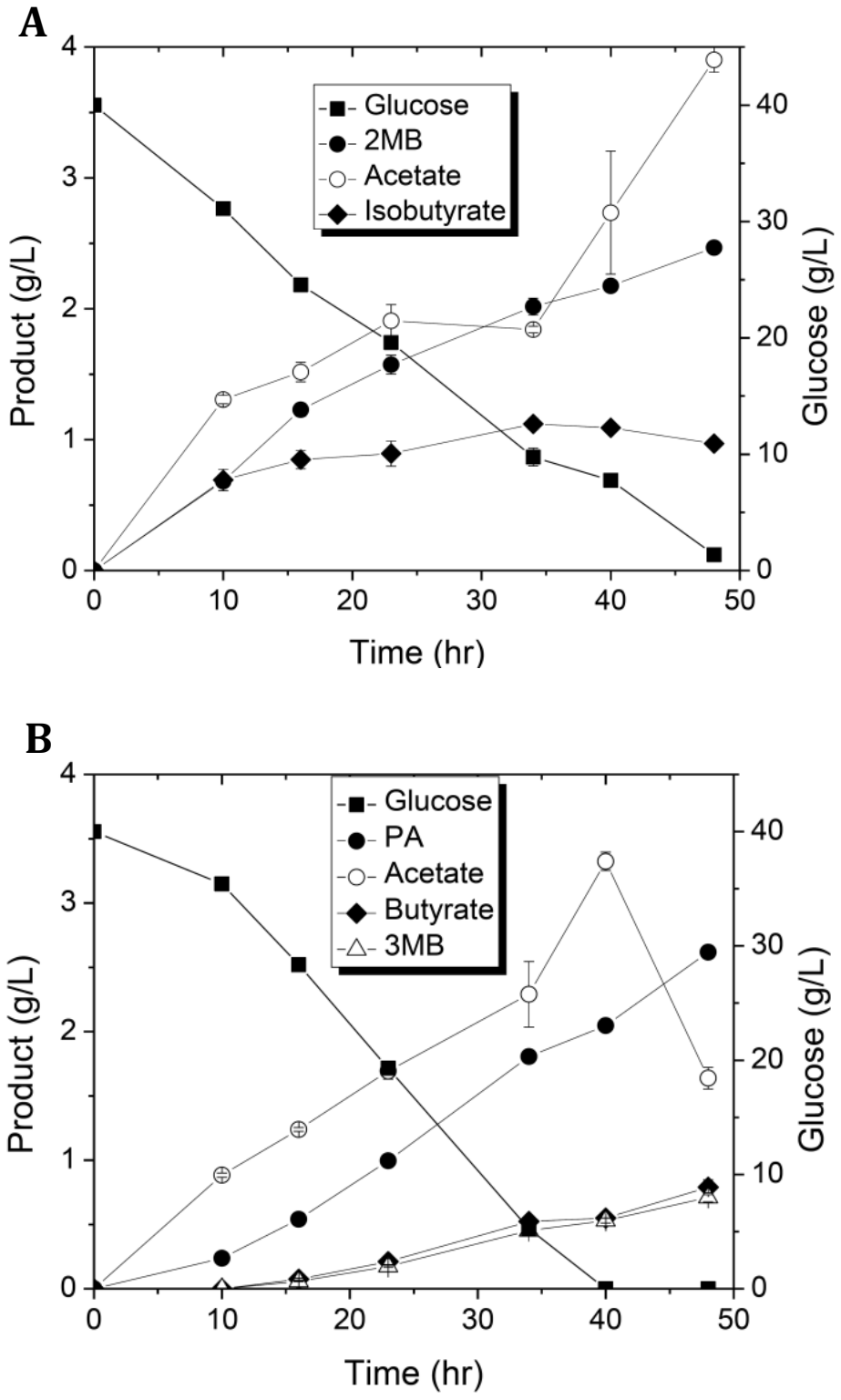

Figure 6: Results of time-course experiments of strains producing 2MB or PA. (A) Time-course measurements of 2MB producing strain. (B) Time-course measurements of PA producing strain.

The production profiles for the final 2MB and PA producing strains are shown in Figure 6. The theoretical maximum yields of PA and 2MB for the designed pathway are 0.28 and 0.38 g per g of glucose. The production values reported here correspond to the yields of 22% and 17% of theoretical maximum for PA and 2MB respectively. The low yields of target compounds are caused by the presence of several byproducts that are formed during the production experiments.

Isobutyrate (IBA) is produced during the production of 2MB due to the action of ilvGMCD operon on pyruvate as a part of valine synthesis pathway. AldH was previously shown to have activity for oxidation of isobutyraldehyde to IBA [40]. The strain exhibits initial high rate of production of both 2MB and IBA. However, it is also accompanied by a high rate of production of acetate. Acetate production can be attributed to the overflow mechanism [74, 75] due to high glucose consumption rate. Under these conditions, the flux through glycolysis is typically much greater than the flux though TCA. This leads to accumulation of intermediates such as pyruvate and acetyl-coA ultimately leading to acetate production. Acetate accumulation inhibits cell growth which results into lower production and glucose consumption rates as can be seen in Figure 6 at later stages in the experiment. The final C4-C5 acid content of the medium was 3.4 g/L which is approximately 9% of glucose supplied.

Production of PA resulted in the production of acetate as well as butyrate and 3-methylbutyrate (3MB). Butyrate is produced from the conversion of 2-ketovalerate intermediate in the PA synthesis pathway. IPDC and KDH_{ba} are known to convert 2-ketoisocaproate (KIC), an intermediate of the leucine synthesis pathway, into 3MB with a

very high activity [41]. Glucose was found to be completely consumed at 40 h, however the production continued to increase. The acetate levels decreased during this period which suggests the action of acetate cycling mechanism in the absence of glucose as carbon source [74]. The total C4-C5 acid content was 4.1 g/L which is slightly higher than in case of 2MB due to lower acetate. The higher rate of glucose consumption may be attributed to the higher catalytic rates (shown in Table 2) achieved by DH in PA production compared to 2MB; however, the rate limiting step appears to be the oxidation in 2MB synthesis and decarboxylation in PA synthesis assuming that the native reactions are faster than these. Another, possibly more important, contributing factor to this can be the fact that the pathway to PA is longer than 2MB, and it consumes an additional acetyl-coA molecule. This can cause a larger fraction of carbon received from glycolysis to go through the synthetic pathway.

Enzyme characterization

In vitro kinetic assays were carried out to confirm the activities of purified enzymes on respective substrates. The kinetic parameters were measured by monitoring the NADH absorbance at 340 nm. The activity of IPDC was measured using a coupled enzyme assay method [39]. The values for the catalytic rate constant (k_{cat}) and Michaelis-Menten constant (K_M) are given in Table 2. The K_M and k_{cat} of IPDC for 2-keto-3-methylvalerate were determined to be 0.85 mM and 4.1 s^{-1}, while the K_M and k_{cat} for 2-ketocaproate were 0.63 mM and 1.9 s-1 respectively. The catalytic efficiency (k_{cat}/K_M) of IPDC for both the substrates was found to be very close. The K_M and k_{cat} of AldH for 2-methyl butyraldehyde were found to be 1.9 mM and 3.6 s^{-1} respectively. KDH_{ba} has significantly lower K_M towards valeraldehyde (0.03 mM) than smaller or branched substrates like

isobutyraldehyde (35 mM) and isovaleraldehyde (7.6 mM) but similar k_{cat} values [41]. Therefore, the catalytic efficiency (k_{cat}/K_M) of KDH_{ba} towards valeraldehyde is 1300-fold and 300-fold higher than those toward isobutyraldehyde and isovaleraldehyde. This can explain why KDH_{ba} worked best for production of the linear long-chain compound, PA.

Table 2: Kinetic parameters for enzymes

Enzyme	**Substrate**	**K_M (mM)**	**k_{cat} (s^{-1})**	**k_{cat}/K_M**
IPDC	2-keto-3-methylvalerate	0.85 ± 0.18	4.1 ± 0.21	4.9
AldH	2-methylbutyraldehyde	1.9 ± 0.24	3.6 ± 0.17	1.9
IPDC	2-ketocaproate	0.6 ± 0.1	1.9 ± 0.06	3
KDH_{ba}	valeraldehyde	0.03 ± 0.01	8.7 ± 0.26	290

Chapter 3

Hydroxylation of Short-Chain Carboxylic Acids

In chapter 2, a biosynthetic approach to production of five-carbon monocarboxylic acids from glucose was discussed. In addition to valerate and 2-methylbutyrate, biosynthesis of other acids such as isobutyrate, 3-methylbutyrate and 4-methylvalerate has been demonstrated in our lab previously [40, 41]. These acids are important intermediates for the chemical industry with applications in making a wide variety of chemicals. One such application is the production of hydroxyacids. This chapter will describe an effort to engineer P450 BM-3 for the hydroxylation of short-chain chain acids with the goal of using it in the metabolic production of hydroxyacids.

Several P450 BM-3 mutants L181K, L181K/L75T, and L181K/F87A mutants are described in the literature [59] to have increased activity on acids with shorter chains. These mutants were used to carry out whole cell biotransformation of 3-methylbutyrate, caproate, and other acids in *E. coli*. However, the HPLC analysis of the samples showed no detectable products as well as no significant consumption of carboxylic acids after 24 hours. *E. coli* has been shown to be capable of using carboxylic acids as the sole source of carbon for growth [76], so it can be expected that it is also capable of importing the acids studied when supplied in a growth medium. This suggests that the lack of hydroxylation activity is not associated with the transport of these acids. So it was concluded that the activity of these mutants is too low to obtain detectable amounts of hydroxylated products. The mutants were analyzed at the molecular level with ROSETTA macromolecular modeling software [77, 78] with the aim of gaining insights

into the mechanism behind increased activity over wild-type and guiding further experiments. More details are presented as Supplementary Data at the end of this document.

Rational engineering of the substrate binding site of P450 BM-3

To change the substrate specificity of P450 from long-chain to short-chain acids, a rational approach to protein engineering was taken. It is known that the residues R47 and Y51 participate in hydrogen bonding interactions with the carboxyl group of the substrate in the binding site [79]. The rest of the binding site is predominantly hydrophobic, which has facilitated the engineering of this protein to allow hydroxylation of a wide range of substrates [80]. The hydrophobic nature of the binding site enables the protein to accept mutations that change the existing hydrophobic residue to any of the other possible hydrophobic residues in the binding site without much loss of stability. This makes it possible to re-engineer the binding pocket to fit a particular substrate. Ost et al. (2000) attempted to design a dyad similar to R47/Y51 closer to the smaller substrate to stabilize carboxylic groups by forming hydrogen bonds. The mutations L181K and L75T were performed to achieve this goal and the mutants were shown to have improved activities on four to eight-carbon substrates. However, a preliminary analysis of L181K mutant with ROSETTA Macromolecular Modeling Suite suggested that K181 may not be involved in stabilization of the carboxyl group (see Supplementary Figure 6). After further analysis of the protein crystal structure, residues A74 and L437 were selected for redesign. The substrate binding site of P450 with the key residues is shown in Figure 7. The side-chains of these residues, unlike L181, point directly towards the substrate as seen from the figure. In addition, the residue A328 has been previously shown to be

important, affecting the binding affinity [81] as well as the regioselectivity of hydroxylation. Each of these residues (A74, A328, and L437) was changed to three different residues (S, H, K) of varying sizes. At positions 74 and 437, the ability of these residues to form hydrogen bonds can stabilize the carboxyl group of the substrate. This resulted in nine P450 mutants. The L181K mutant described in the literature by Ost et al. (2000) was also created for comparison with these nine mutants and the wild-type.

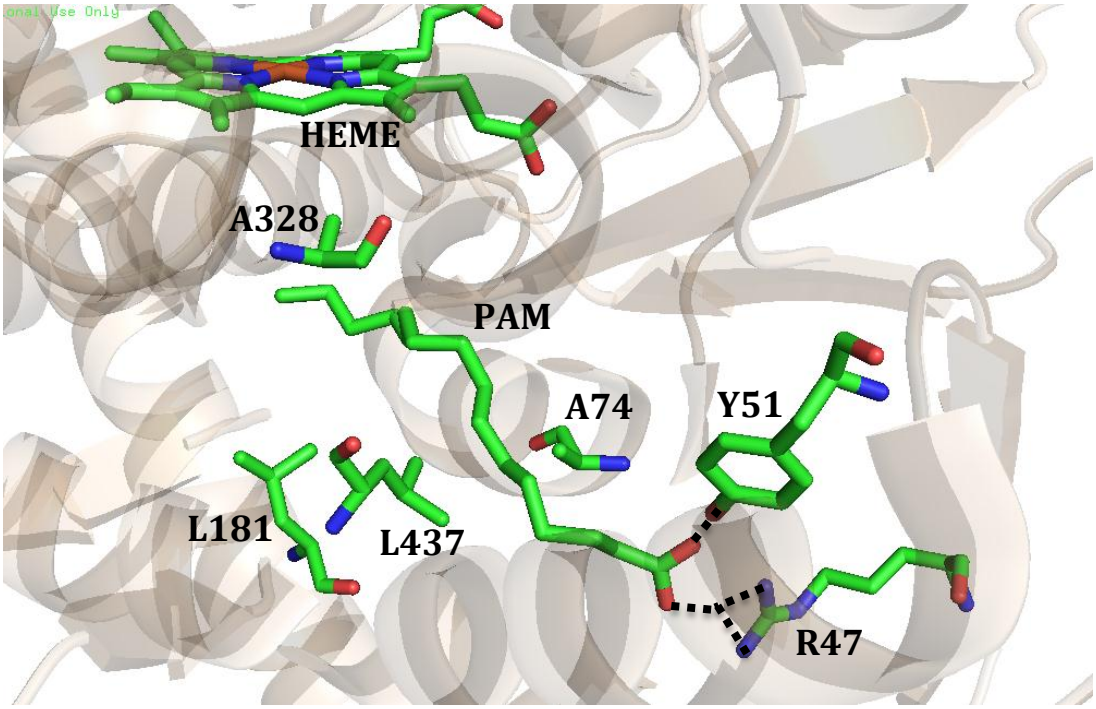

Figure 7: The crystal structure of P450 BM-3 (PDB ID: 2UWH) showing the substrate binding site occupied by palmitic acid (PAM). Single letter amino acid codes (Alanine, A; Leucine, L, Arginine, R; Tyrosine, Y) are used with numbers indicating the position of the residues on the protein chain. The dotted lines are cartoon representations of the hydrogen bonding interactions of R47 and Y51 with the carboxyl group. The carbon atoms are shown in green, nitrogen atoms in blue, and oxygen atoms in red. The image was created using PyMOL.

Activity measurements of P450 mutants

The nine mutants described earlier, along with L181K mutant described in the literature and wild-type P450 were analyzed for their activity on various short-chain carboxylic acid substrates. The substrates selected for this study were valerate (C5), 2-methylbutyrate (2MB), 3-methylbutyrate (3MB), caproate (C6), and 4-methylvalerate (4MV). All of these, except the C6 can be biologically derived from glucose as previously demonstrated in our lab. The activities were measured in cell extracts by supplying with a fixed amount of each substrate individually with the cofactor NADPH. The decrease in absorbance of NADPH at 340 nm was monitored and used to calculate rates. The protocols for preparation of cell extracts and the kinetic assays are described in chapter 4. The total protein concentrations were measured by the Bradford assay and used to normalize measured rates to account for variations in cell extract preparation. The rates were expressed as relative values with respect to wild-type activity for comparison of different mutants on the same substrate.

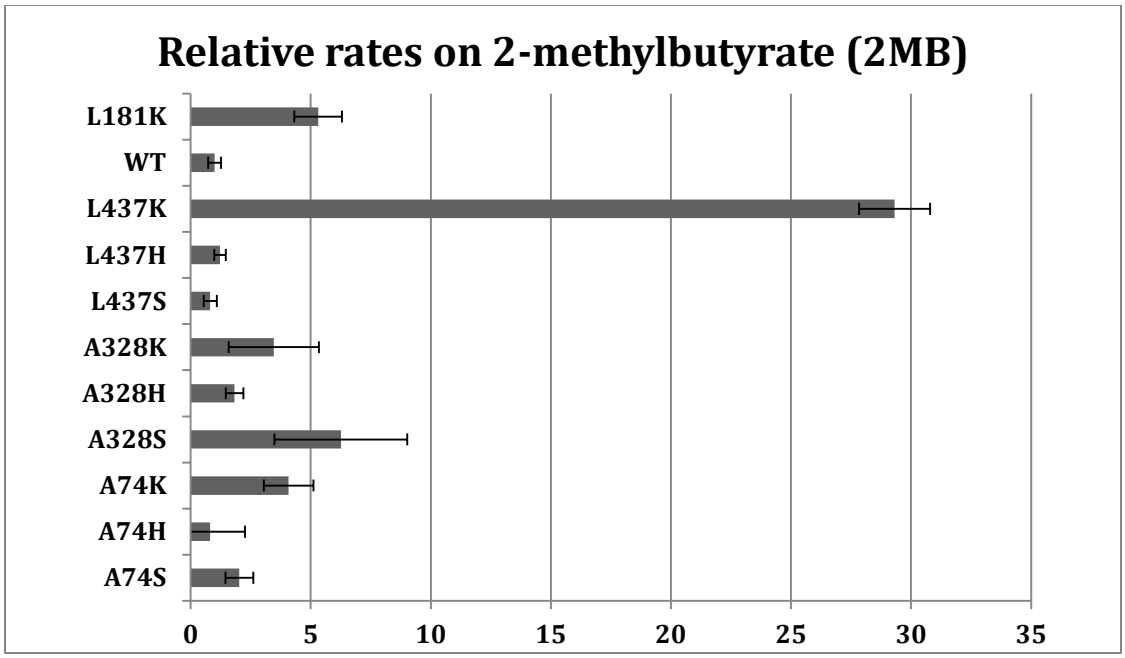

Figure 8: Rates relative to wild-type P450 on 2-methylbutyrate (2MB) as determined in the cell extract assays. Errors bars indicate the standard error (n=3).

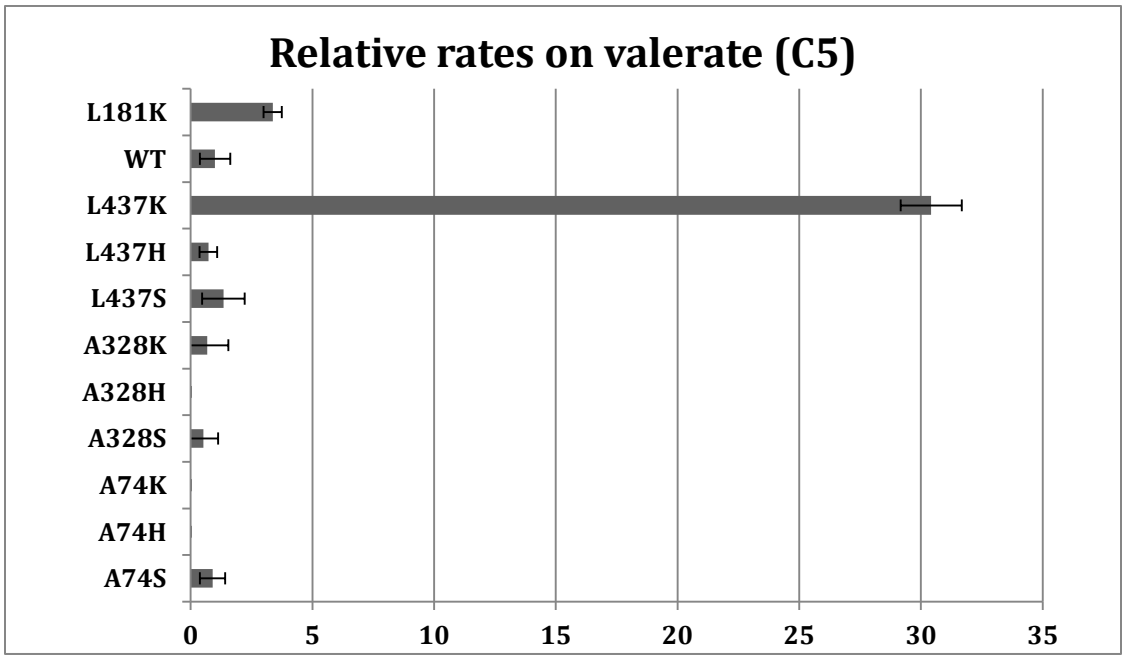

Figure 9: Rates relative to wild-type P450 on valerate (C5) as determined in the cell extract assays. Errors bars indicate the standard error (n=3).

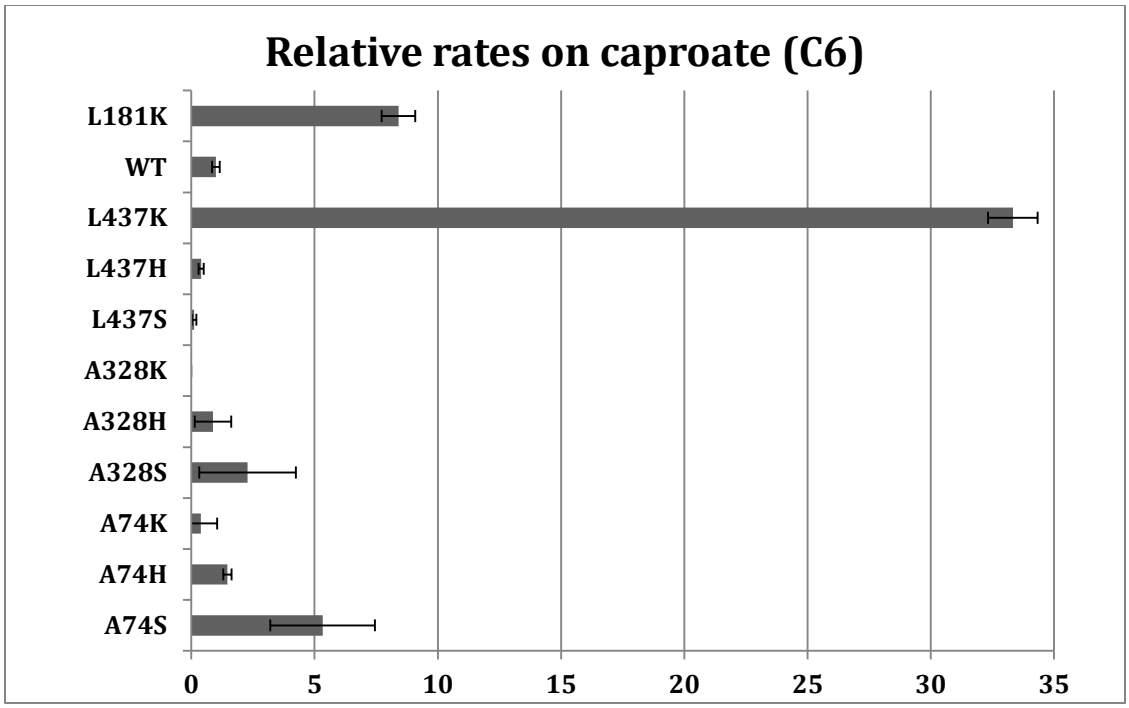

Figure 10: Rates relative to wild-type P450 on caproate (C6) as determined in the cell extract assays. Errors bars indicate the standard error (n=3).

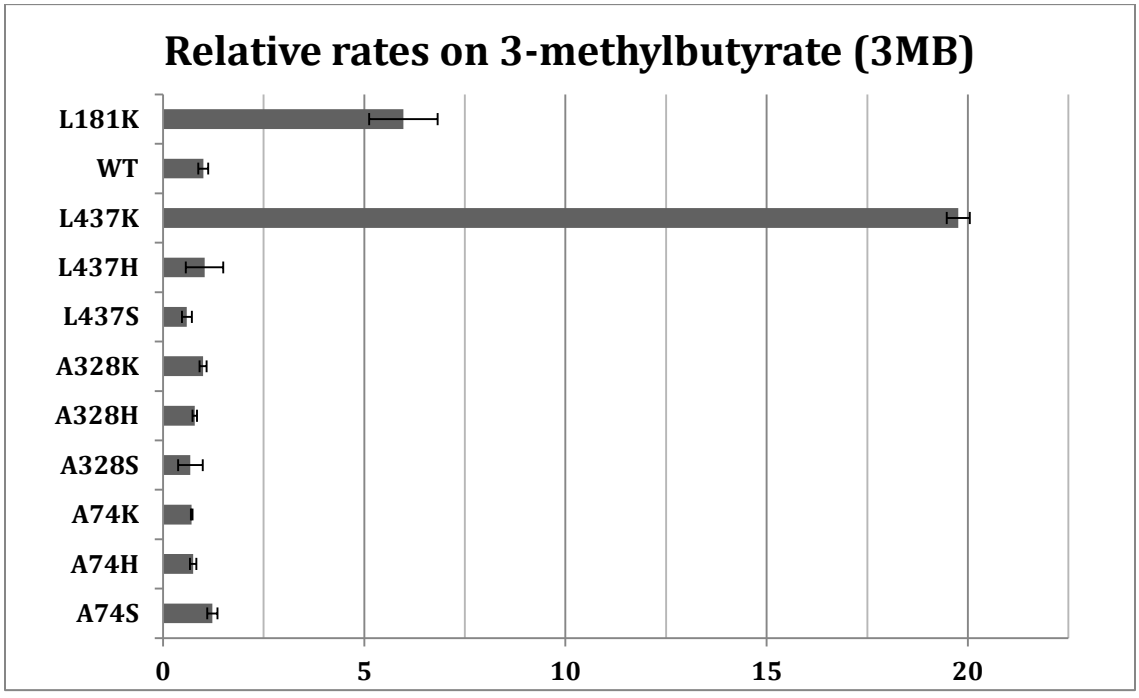

Figure 11: Rates relative to wild-type P450 on 3-methylbutyrate (3MB) as determined in the cell extract assays. Errors bars indicate the standard error (n=3).

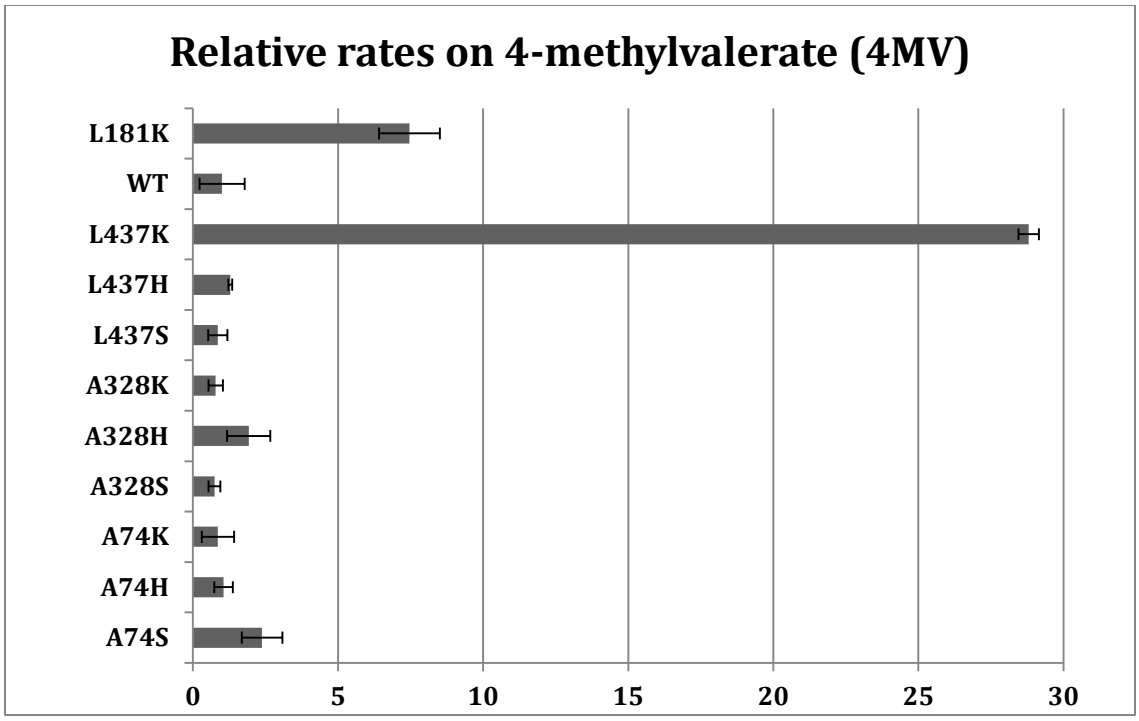

Figure 12: Rates relative to wild-type P450 on 4-methylvalerate (4MV) as determined in the cell extract assays. Errors bars indicate the standard error (n=3).

The mutant L437K has the highest normalized activity for all the substrates studied as seen from figures 8 to 12. The mutant A74S also has higher activity than the wild-type for six-carbon substrates C6 and 4MV. However, it fails to do better than wild-type for the small five-carbon substrates. The serine side-chain in A74S mutant is small and thus may not be effective in stabilizing smaller substrates for which the carboxyl groups are further away from the hydroxyl group of serine.

Figure 13 shows absolutes rates measured in moles of NADPH consumed per minute per milligram of total protein as determined by Bradford assay. The absolute rates are useful for comparison of activities across various substrates. It is clear from the figure that all

mutants show a lower activity on C5 compared to C6. This is to be expected since the enzyme naturally favors longer substrate. Interestingly, it is observed that in case of five-carbon acids, the branched chain 3MB and 2MB molecules have higher rates of conversion for L181K. In case of six-carbon molecules, the branched 4MV does not show higher rate than the linear C6, but the difference is not statistically significant ($p=0.22$). This result is interesting because the branched chain molecule has a shorter chain length and thus should have a lower conversion rate. The effect of the chain length can be attributed to the hydrogen bonding interactions, while the effect of branching may be due to the hydrophobic interactions. It may explain why there is a statistically significant increase in the activity of L181K but not L437K on branched chain molecules. This is consistent with the hypothesis that L437K is involved in forming hydrogen bonds with the carboxyl group while L181K affects rate via a different mechanism. It has been shown earlier that the mutation A328V enhances binding of native substrates to the enzyme. This mutation leads to a decreased binding pocket size near the heme group. It is possible that a similar effect is in action when a branched chain acid is present in the active site. It can also explain the higher activity on 3MB compared to 2MB since the methyl side group in 3MB is further close to the heme group than in 2MB.

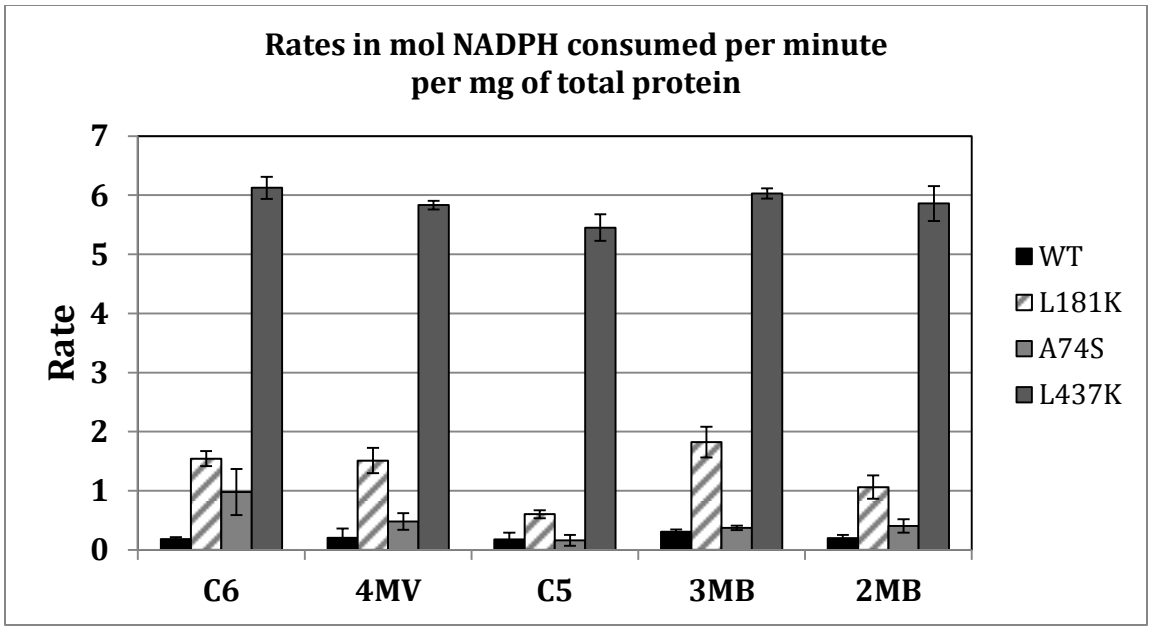

Figure 13: Absolute rates as determined by the cell extract assays on various substrates- caproate (C6), 4-methylvalerate (4MV), valerate (C5), 3-methylbutyrate (3MB), and 2-methylbutyrate (2MB).

Studies with double mutants of P450s

In the previous section, two beneficial mutations were identified in addition to the mutation L181K reported in Ost et al. (2000). These mutations (A74S and L437K) were individually combined with L181K to generate double mutants of P450. The hypothesis was that their combination could result in increased activities. However, the assay with cell extracts indicated a lower activity of these mutants than the individual L181K mutation. This was the case with all the substrates tested. The results are shown in Figure 14. This might be the result of destabilization due to charge burial. In case of mutations that do not conserve charge, the additional charge needs to be stabilized. In earlier case, the carboxylic group was able to perform this function, but it may not be the case with double mutants. This needs further inspection.

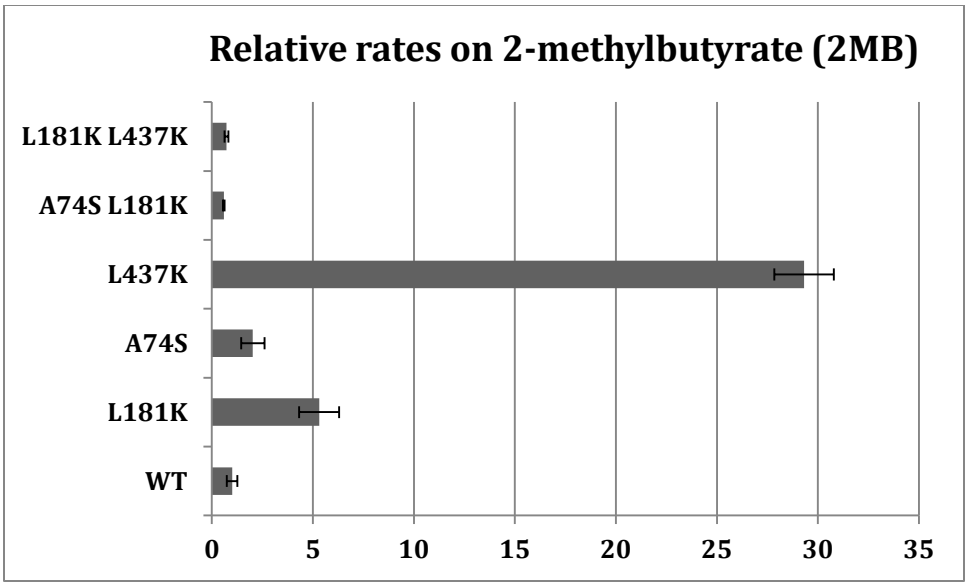

Figure 14: Rates relative to wild-type P450 on caproate (C6) as determined in the cell extract assays. Errors bars indicate the standard error (n=3).

Biosynthetic strategy for hydroxyisobutyrate

In chapter 1, 3-hydroxyisobutyrate was identified as an important building block for the chemical industry with many applications. It can be synthesized by hydroxylating isobutyrate. However, an isobutyrate-hydroxylating enzyme or pathway is not known. So it was critical to discover or design a system capable of carrying out this transformation. A screening method was developed to aid the discovery of such a system.

The screening method was based on the valine degradation pathway in which HIBA is converted into propanoyl-CoA [82]. *E. coli* has been shown to grow on propionate previously [83, 84]. Inside the cell, propanoyl-CoA is oxidized to pyruvate which is then converted to all the essentials compounds required for cell growth. Propanoyl-coA enters the central metabolism to support growth (Figure 15). In this pathway, 3-

hydroxyisobutyrate is oxidized to methylmalonate-semialdehyde by 3-hydroxyisobutyrate dehydrogenase (MmsB). Finally, the aldehyde is converted to propanoyl-CoA by methylmalonate-semialdehyde dehydrogenase (MmsA) [85]. The *mmsA-mmsB* operon from *Pseudomonas aeruginosa* [86], *Pseudomonas putida* KT2440, and *Bacillus subtilis* were cloned in *E. coli* and checked for their ability to perform the desired function.

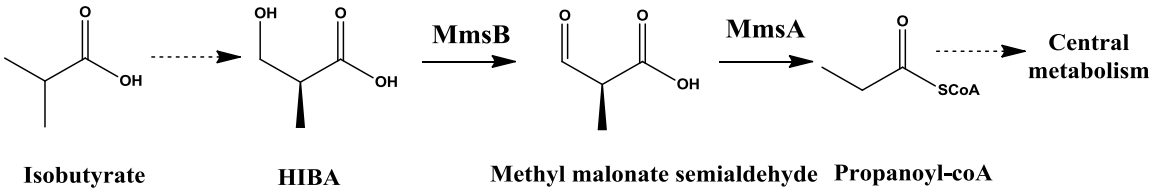

Figure 15: Growth based screening strategy for isobutyrate-hydroxylating P450.

Growth assays on 3-hydroxyisobutyrate

The cells expressing mmsAB operon from *P. aeruginosa* showed weak growth (visible growth only after 72 hours of incubation in a sealed tube) on HIBA as the sole carbon source in M9 minimal medium. The growth assay was performed three times to ensure consistency of results. Figure 16 shows the picture taken after one of these experiments. Considering that the P450 mutants also have low activities on isobutyrate, the growth assay was not found to be very useful with the mutants in hand. It is still a promising tool that will be extremely valuable when a suitable P450 mutant library is developed or another hydroxylase is discovered. As a growth-based selection strategy, it will allow screening of a large library.

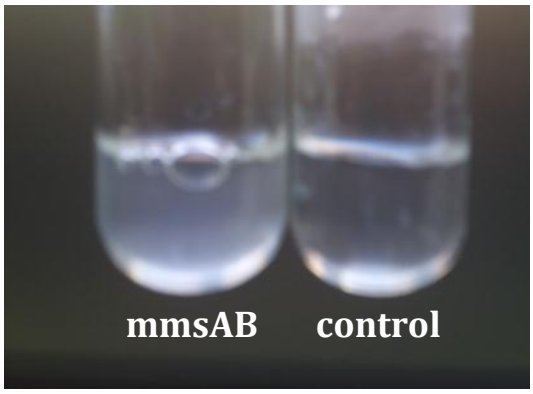

Figure 16: Growth assay for mmsAB expressing *E. coli* cells on HIBA (2 g/L). The tube containing mmsAB expressing *E. coli* shows higher turbidity indicating growth. The OD_{600} was 0.14 for mmsAB sample and non-detectable for the control.

The weak growth observed in the assay could be the result of poor protein expression due to different codon usage between *E. coli* and *P. aeruginosa*. Before using the assay for screening of mutant library, this will need to be addressed by either codon optimization or by increasing the copy number.

Chapter 4

Conclusion and Future Directions

The native leucine and isoleucine biosynthetic pathways in *E. coli* were successfully expanded for the synthesis of pentanoic acid and 2-methylbutyric acid respectively. Several aldehyde dehydrogenases and 2-ketoacid decarboxylases were studied for the conversion of ketoacids into respective carboxylic acids. The optimal combinations of these enzymes enabled production of 2.6 g/L 2MB with IPDC-AldH and 2.6 g/L of PA with IPDC-KDH_{ba}. These values correspond to the yields of 22% and 17% of theoretical maximum for PA and 2MB respectively. In vitro enzymatic assays confirmed the activities of these enzymes on the nonnatural substrates studied. To the best of author's knowledge, this is the earliest report of metabolic engineering for the synthesis of C5 monocarboxylic acids. The natural environments in which these acids have been observed previously are anaerobic. This work demonstrates an aerobic process for the production of these acids. The PA producing strain exhibited a higher glucose consumption rate than the 2MB producing strain. It can be attributed to the fact that the pathway to PA is longer and consumes an additional acetyl-coA molecule.

The shake flask experiments have shown the presence of significant quantities of acetate. It can be attributed to the overflow mechanism as well as the limited supply of oxygen. These limitations can be overcome in a carefully operated stirred-tank type fed-batch reactor by maintaining low levels of glucose and passing air through the tank to supply oxygen. Future work should be directed towards optimization of the pathways and bioreactor scale-up. The biosynthetic strategy developed in this work adds to the

repertoire of chemicals produced through metabolic manipulation of a host organism. Since the pathways are based on host's native amino acid biosynthetic pathways, a variety of organisms can be explored as hosts after the proof of concept presented in this work.

The cytochrome P450 BM-3 enzyme was studied for its ability to oxidize unactivated C-H bonds in the short-chain carboxylic acids discussed above along with others that were biologically produced in our lab. Nine mutants were created based on the literature, ligand docking analysis using the ROSETTA macromolecular modeling suite and visualization with PyMOL. These nine mutants were compared with the L181K mutant described in the literature and the wild-type enzyme. The mutant L437K was found to have the highest activity (20 to 30-fold higher than wild-type depending on the substrate) based on the cell extract assays. The mutant enzymes L437K and L181K, and the wild-type enzyme were purified and their relative activities were confirmed in vitro. The mutation L181K was combined with mutations L437K and A74S individually to investigate the possibility of an additive or synergistic effect. However, it was observed that the double mutants had lower activities than the L437K mutant in each case. Future analysis should aim to understand the basis of this gain or loss of activity in order to guide further development of P450 as catalysts.

These results are promising for enabling the biosynthesis of renewable hydroxyacid monomers from glucose. Future work should involve understanding the structural effects of individual mutations and their relation to activity. This will facilitate further optimization of the binding site. The L437K mutant should be incorporated in the glucose

to carboxylic acid pathways to demonstrate hydroxyacid synthesis directly from glucose using whole cells. At this point, the regio-selectivity of hydroxylation is not determined. It is expected based on the literature that the hydroxylated products will be a mixture of positional isomers. So it is necessary to characterize the products of hydroxylation.

The mmsAB operon from *P. aeruginosa* was cloned into *E. coli* and it was demonstrated that it enabled growth on 3-hydroxyisobutyrate. This can serve as a growth-based screening strategy for the enzymes capable of hydroxylating isobutyrate to 3-hydroxyisobutyrate. However, the growth on 3-hydroxyisobutyrate was very weak. Considering that the P450 mutants also have low activities on isobutyrate, the growth assay was not found to be very useful with the mutants in hand. It is still a promising tool that will be extremely valuable when a suitable P450 mutant library is developed or another hydroxylase is discovered. As a growth-based selection strategy, it will allow screening of a large library.

The anticipated problems with the biosynthetic routes developed in this work are high costs of separation of products [61] and lowering of pH during the production of acids negatively affecting cell growth [62]. These problems can be addressed by polymerizing the hydroxyacids as soon as they are produced to polyhydroxyalkanoates. Polyhydroxyalkanoates (PHAs) production using microorganisms has gained a lot of attention recently [63, 64]. The pathways developed in this work will expand the scope of PHAs beyond naturally occurring monomers.

Chapter 5

Materials and Methods

Bacterial strains, reagents, media and cultivation

The *E. coli* strain used for production of C5 carboxylic acids was a threonine overproducer strain (ATCC98082) which had threonine and homoserine exporter gene rhtA knocked out to ensure high intracellular levels of threonine [21]. yqhD gene was knocked out from this strain using the P1 phage transduction method. The ΔyqhD Keio strain [87] was used to prepare P1 lysate for use in the knockout procedure. The plasmid pCP20 to remove the kanamycin resistance marker inserted during gene deletion. The various strains and plasmids used in this study are listed in table 1. The final strain (PA1) was transformed with plasmids pIPA1, pIPA2 and any one of the pIPA4 to pIPA15 for production of 2MB. For production of PA, it was transformed with pIPA1, pIPA3 and any one of the plasmids pIPA4 to pIPA15.

XL1-Blue and XL10-Gold competent cells from Stratagene (La Jolla, CA) were used for propagation of plasmids. BL21 (DE3) strain from New England Biolabs (Ipswich, MA) was used for protein expression. All the restriction enzymes, Quick ligation™ kit and Phusion® high-fidelity PCR kit were from New England Biolabs.

A 2xYT rich medium (16 g/L Bacto-tryptone, 10 g/L yeast extract and 5 g/L NaCl) was used to culture the *E. coli* strains at 37°C and 250 rpm unless specified otherwise. Antibiotics were added as needed (100 µg/mL ampicillin, 25 µg/mL kanamycin and 25 µg/mL spectinomycin).

Shake-flask production experiments and HPLC analysis

Production experiments were carried out in triplicates. Three independent colonies were picked from freshly transformed *E. coli* strains and cultured overnight in 2 ml 2xYT medium containing appropriate antibiotics. 250 µl of overnight cultures were transferred into 125 ml conical flasks containing 5 ml M9 medium supplemented with 40 g/L glucose, 5 g/L yeast extract, 10 mg/L thiamine, 100 mg/L ampicillin, 25 mg/L kanamycin and 25 mg/L spectinomycin. Protein expression was induced by adding 0.1 mM isopropyl-β-D-thiogalactoside (IPTG). 0.2 g $CaCO_3$ was added to each flask for neutralization of acids produced and sterilized by autoclaving. After incubation for 48 hours at 30°C and 250 rpm, samples were centrifuged, supernatants were collected and diluted twice for analysis. Analysis was done using an Agilent 1260 Infinity HPLC containing an Aminex HPX 87H column (from Bio-Rad) equipped with a refractive-index detector. The mobile phase was 5 mM H_2SO_4 at a flow rate of 0.6 ml/min. The column temperature was 35°C and detection temperature was 50°C. The loss due to vaporization was estimated to be less than 5%. The data are presented as the mean values with error bars indicating the standard error.

Expression and purification of AldH

For purification of AldH, the gene was cloned into an expression plasmid having N-terminal 6xhis-tag (pIPA16). This plasmid was used for transformation of *E. coli* strain BL21. Cells were inoculated from an overnight pre-culture at 1/300 dilution and grown at 30 °C in 300 ml 2xYT rich medium containing 100 mg/L ampicillin. When the OD reached 0.6, IPTG was added for induction of protein expression. Cell pellets were lysed

by sonication in a buffer (pH 9.0) containing 250 mM NaCl, 2 mM DTT, 5 mM imidazole and 50 mM Tris. The enzyme was purified from crude cell lysate through Ni-NTA column chromatography and buffer-exchanged using Amicon Ultra centrifugal filters (Millipore). 50 µM tris buffer (pH=8), 1 mM $MgSO_4$ and 20% glycerol was used for storage of AldH. 100 µl of concentrated protein solutions were aliquoted into PCR tubes and flash frozen at -80 °C for long term storage. Protein concentration was determined by measuring UV absorbance at 280 nm. Purified KDH_{ba} and IPDC were available from another study [41].

Kinetic assays for AldH, KDH_{ba}, and IPDC

The kinetic assay of KDH_{ba} consisted of 0.5 mM NAD^+ and valeraldehyde in the range of 50 to 400 µM in assay buffer (50 mM NaH_2PO_4, pH 8.0, 1mM DTT) with a total volume of 78 µl. To start the reaction, 2 µl of 1 µM KDH_{ba} was added and generation of NADH was monitored at 340 nm (extinction coefficient, 6.22 mM^{-1} cm^{-1}) at room temperature. Similar protocol was used for AldH with 2-methylbutyraldehyde concentrations in the range of 1 to 6 mM.

The activity of IPDC was measured using a coupled enzymatic assay method. Excess of appropriate aldehyde dehydrogenase (AldH for 2-keto-3-methylvalerate and KDH_{ba} for 2-ketocaproate) was used to oxidize aldehyde into acid while cofactor NAD^+ was reduced to NADH. The assay mixture contained 0.5 mM NAD^+, 0.1 µM appropriate aldehyde dehydrogenase and corresponding 2-keto acid in the range of 1 to 8 mM in assay buffer (50 mM NaH_2PO_4, pH 6.8, 1 mM $MgSO_4$, 0.5 mM ThDP) with a total volume of 78 µl. To start the reaction, 2 µl of 1 µM IPDC was added and generation of NADH was

monitored at 340 nm. Kinetic parameters (k_{cat} and K_M) were determined by fitting initial rate data to the Michaelis–Menten equation.

Cloning of cytochrome P450 BM-3 and its mutants

The *Bacillus megaterium* strain was used as the source of genomic DNA for amplification of cytochrome P540 BM-3. The -80 °C frozen stock of this strain was inoculated in 2mL of LB and cultured for 5 to 7 hours. 50 to 100 μL of this culture was incubated at 98 °C for 5 to 10 minutes and then centrifuged. The supernatant from this process was used in the polymerase chain reaction (PCR) as the source of genomic DNA. A silent mutation was performed in the P450 sequence using primers P2 and P3 to introduce an XbaI restriction site to facilitate further cloning of mutant sequences. The PCR products were gel purified and ligated by the Gibson assembly protocol. The ligation mixture (total volume = 5 μL) was used for transformation of 100 μL of XL10 gold chemical competent cells. The cells were spread immediately on LB agar plates and incubated overnight at 37 °C. Several colonies were picked from the plate and cultured for 6 to 8 hours in 2 mL LB supplemented with ampicillin. Plasmid DNA was purified from each culture using the Zyppy™ Plasmid Miniprep Kit available from Zymo Research (Irvine, CA) and successful clones were verified by enzyme digestion. P450 mutant sequences were created by PCR site-directed mutagenesis using appropriate primers listed in table .The insert region was verified by DNA sequencing from Eurofins MWG Operon.

Expression of P450s and preparation of cell extracts

The P450 mutants were expressed in *E. coli* strain BL21. BL21 was inoculated into LB from -80 °C frozen stock and cultured at 37 °C for 6 to 8 hours. The cells were then harvested by centrifuging and washed twice with deionized, sterilized cold water. The cells were finally resuspended in 10% glycerol and transformed by electroporation. 100 µL of cells were mixed with 0.5 µL of plasmid DNA and transferred to an electroporation cuvette. After electroporation, cells were spread on ampicillin containing agar plates and incubated overnight at 37 °C. A single colony was picked from each plate and cultured for 6 to 8 hours in LB before making a -80 °C frozen stock containing 20% glycerol for future use.

For expression of P450, 2 mL LB containing ampicillin was inoculated with P450 mutant strain from -80 °C frozen stock and cultured at 37 °C for 5 to 6 hours. 2.5 µg cells (wet cell mass) from each of this pre-culture was then inoculated in 3 mL of terrific broth (TB) supplemented with 100 µg/mL ampicillin, 1000-fold dilution of a stock solution of trace minerals, 0.5 mM δ-aminolevulinic acid (δ-ALA) in 15 mL falcon tubes. TB contained 12 g/L tryptone, 24 g/L yeast extract, 0.4 % (v/v) glycerol, 17 mM KH_2PO_4, and 72 mM K_2HPO_4 in deionized water. 1000X trace minerals solution contained 50 mg $MgCl_2$, 2.5 g $FeCl_2.4H_2O$, 100 mg $ZnCl_2.4H_2O$, 20 mg $CoCl_2.6H_2O$, 100 mg $Na_2MoO_4.2H_2O$, 50 mg $CaCl_2.H_2O$, 100 mg $CuCl_2$, 20 mg H_2BO_3, 10 mL concentrated HCl (37%) in a total volume of 100 mL. This culture was incubated at 30 °C for two hours before induction of protein expression by addition of 0.5 mM IPTG. The protein expression was continued overnight, typically for 14 to 16 hours. The cells were pelleted by centrifuging for 5 minutes at 3220 g. The cell pellets were stored at -80 °C until further use.

For preparation of cell extracts, the frozen cell pellets were first thawed on ice-water mixture and resuspended in 600 µL of lysis buffer. The lysis buffer contained 1 mg/mL lysozyme, 10 mM $MgCl_2$, 1 mM phenylmethylsulfonyl fluoride (PMSF), 2 U/mL DNAseI in 100 mM phosphate buffer (pH=8). PMSF was added from a 200 mM stock in isopropanol. 100 mM phosphate buffer (pH=8) was prepared by dissolving 0.1 g $NaH_2PO_4.H_2O$ and 2.5 g $Na_2HPO_4.7H_2O$ in 100 mL deionized, sterilized water. The resuspended cells were incubated at 37 °C for 1 hour to allow lysis to proceed. The lysed cells were centrifuged for 15 minutes at 3220 g and supernatants were collected as cell extracts for use in activity assays.

Cell extract activity assays for P450 mutants

The activity assays were performed in 96-well UV transparent plates. The assay mixture contained 56 µL of 100 mM phosphate buffer (pH=8), 10 µL of 80 mM substrate, 4 µL cell extract. The reaction was initiated by adding 10 µL of 5 mM NADPH. All the stock solutions were prepared in 100 mM phosphate buffer (pH=8). The rates were determined by measuring the decrease in absorbance at 340 nm due to consumption of NADPH. The total assay volume was 80 µL which corresponded to a path length of 0.5 cm. The negative controls (no substrate, no NADPH or no cell extract) were included for some of the initial assays to ensure that the observed NADPH consumption was due to reaction of the substrate by P450. The background for NADPH consumption in cell extracts was measured with cell extracts prepared from BL21 strain without the P450 plasmid. This background NADPH consumption rate was subtracted from the rated measured for P450 mutants. The rates were normalized by the total protein content of each cell extract (as determined by Bradford assay) to account for variability in cell extract preparation. For

comparison purposes, the activity of wild-type P450 was arbitrarily set to 1.0 for each substrate and the activities of other mutants were calculated as rates relative to wild-type P450.

Bradford assay

The Bradford assay consisted of 4 µL of sample with 200 µL of Quick Start Bradford 1x Dye Reagent (from Bio-Rad). The mixture was incubated for 10 minutes and the absorbance was measured at 595 nm. The concentration of total protein was determined by comparing with standards prepared by diluting BSA to appropriate amounts. For the determination of standard curves, 0.25 to 1 mg/mL of BSA was added to each well and incubated for at least 10 minutes with 200 µL of Bradford reagent. The concentration v/s absorbance data was fitted to a straight line and used to determine concentrations in unknown samples.

Purification of P450s

The BL21 *E. coli* strain transformed with the P450 to be purified was inoculated from the -80 °C frozen stock into 2 mL LB containing ampicillin. The cultures were incubated at 37 °C for 5 to 6 hours. 250 µL of this pre-culture was inoculated in 5 mL TB supplemented with 100 µg/ml of ampicillin, 1000-fold dilution of a stock solution of trace minerals, and 0.5 mM δ-ALA. 1 mL of this culture was inoculated into 250 mL of TB supplemented with ampicillin, trace minerals and δ-ALA in the same proportions as the previous culture. The culture was incubated for 2 hours at 37 °C before addition of 0.5 mM IPTG and was then transferred to 30 °C for overnight incubation. The cells were

pelleted by centrifuging at 3220 g for 10 minutes. The supernatants were discarded and the pellets were stored at -80 °C until further use.

For lysis, the cell pellets were first thawed on ice-water mixture and resuspended in 25 mL of lysis buffer. The lysis buffer (pH=7.6) contained 50 mM Tris-HCl, 100 mM NaCl, 5% glycerol, 1 mM DTT and 1 mM PMSF. Cell lysis was performed by sonication using the Heat Systems Ultrasonics W-225 Sonicator in a continuous mode set at 50% duty cycle and output control 5. Each sample was sonicated for 3 minutes with intermittent cooling on ice-water mixture. The cell lysates were centrifuged at 3220 g for 40 minutes followed by 11000 g for 15 minutes.

4 mL of HisPur Ni-NTA resin solution (available from Thermo Scientific) was loaded in each column and the storage buffer was allowed to pass through to get 2 mL final resin bed volume. The resin was equilibrated with 7 mL of lysis buffer and drained. 25 mL of cell lysate was loaded in the column and allowed to pass through by gravity. The column was then washed twice with 20 mL of wash buffer (50 mM Tris-HCl, 100 mM NaCl, and 20 mM imidazole). The bound protein was eluted with 15 mL of elution buffer (pH=8) which contained 50 mM Tris-HCl, 250 mM NaCl, and 250 mM imidazole. The final protein sample was then buffer-exchanged using Amicon Ultra centrifugal filters (Millipore) with the storage buffer (100 mM phosphate buffer, 20% glecerol, pH=8) to a final 100-fold dilution of the elution buffer.

Chapter 6

Supplementary Data

Kinetics data and fit to Michaelis-Menten model

The data were collected as described in chapter 4. The initial rates were fitted to the Machialis-Menten unimolecular model assuming complete saturation with NAD^+ cofactor. The data were collected as triplicates and are presenetd as mean with error bars indicating standard error.

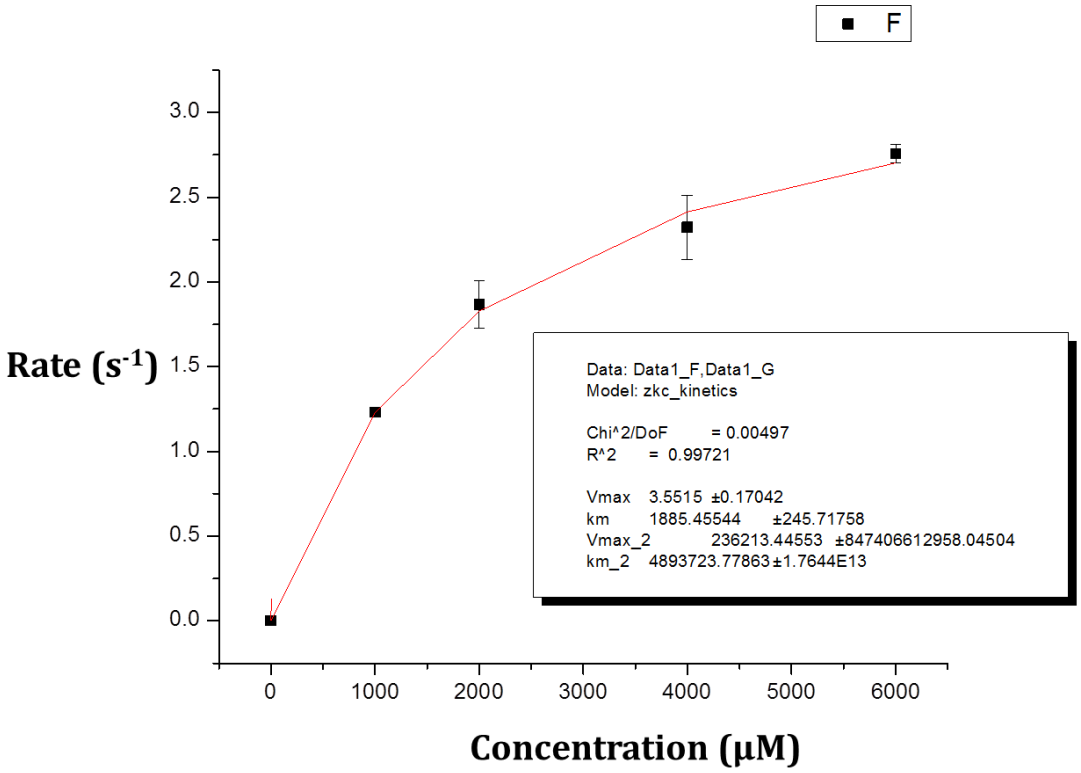

Supplementary Figure 1: Kinetics of AldH on 2-methylbutyrate.

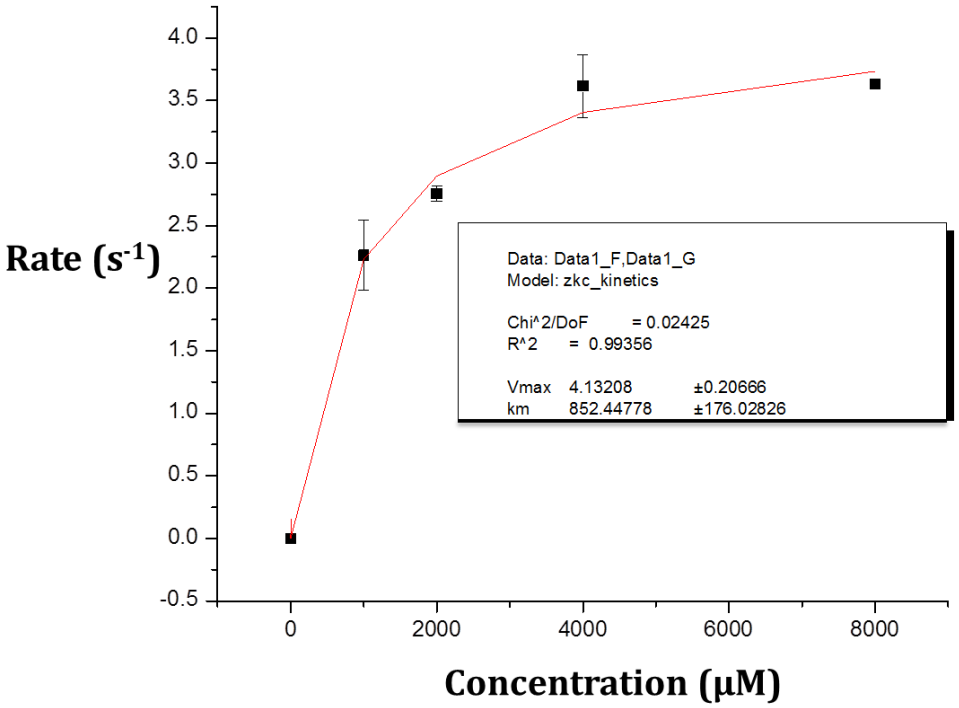

Supplementary Figure 2: Kinetics of IPDC on 2-keto-3-methylvalerate.

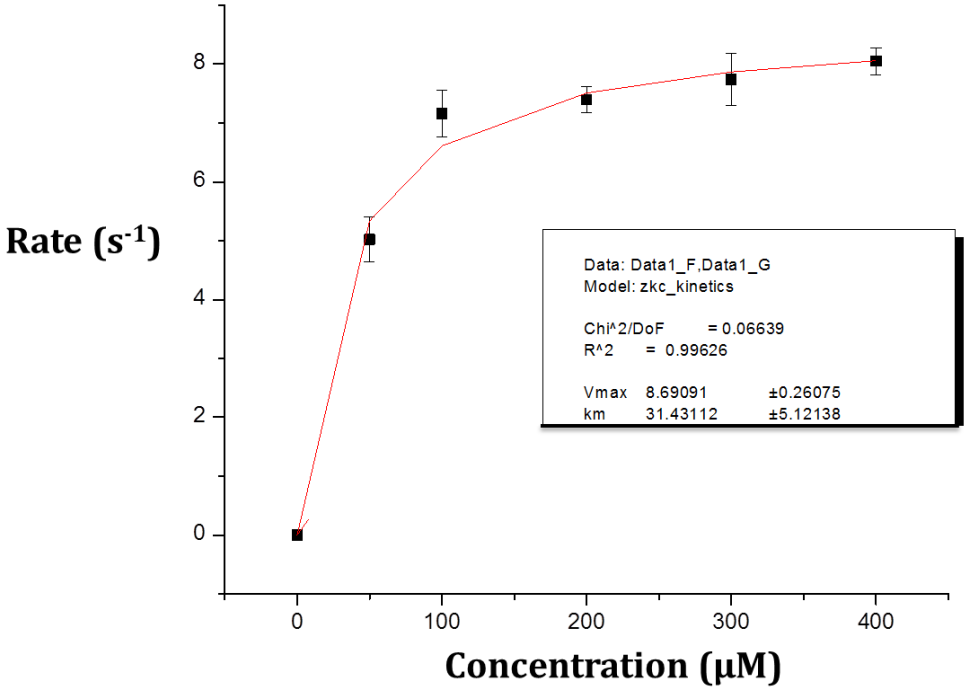

Supplementary Figure 3: Kinetics of KDH_{ba} on pentanoic acid.

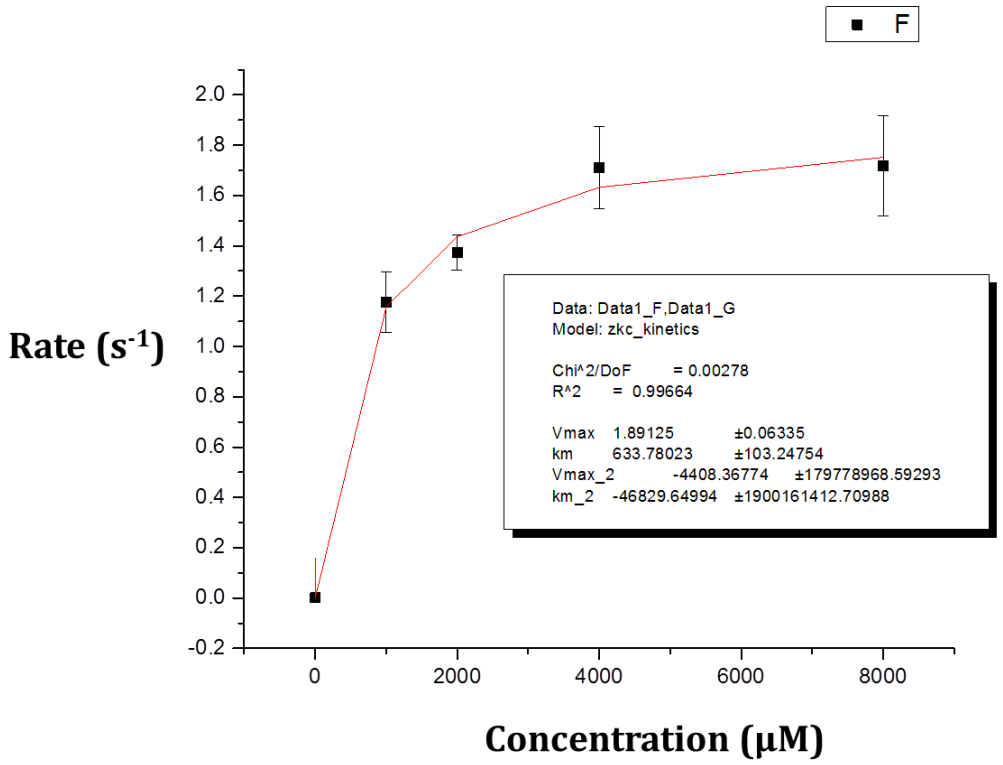

Supplementary Figure 4: Kinetics of IPDC on 2-ketocaproate.

Docking ligands onto P450 using ROSETTA

The crystal structures of WT P450 bound to its substrates are available from the Protein Databank. As a proof of concept, the binding conformation of N-palmitoyl glycine to the enzyme was computed using ROSETTA macromolecular modeling software and compared to the native structure. Supplementary Figure 5 shows the initial random placement of the substrate during modeling (A), the predicted conformation after the ligand docking application in ROSETTA (B) and the experimental structure obtained by crystallography (C). The algorithm adopts a Monte Carlo approach to minimize the energy of the complex. 1400 models were created for this purpose and they were later

ranked to find the models associated with low overall and low binding energy to find the predicted conformation. An example of modeling parameters used is given below to facilitate reproduction of these results.

```
-in
 -file
  -s L181K_A_HEM_DKA_0001.pdb
-extra_res_fa DKA.params HEM.params
-out
 -nstruct 200
 -file
  -silent L181K_silent.out
-packing
 -no_optH false
 -ex1
 -ex1aro
 -ex2
 -extrachi_cutoff 1
-docking
 -uniform_trans 5
 -ligand
  -improve_orientation 1000
  -minimize_ligand
  -harmonic_torsions 10
  -minimize_backbone
  -harmonic_Calphas 0.3
  -soft_rep
```

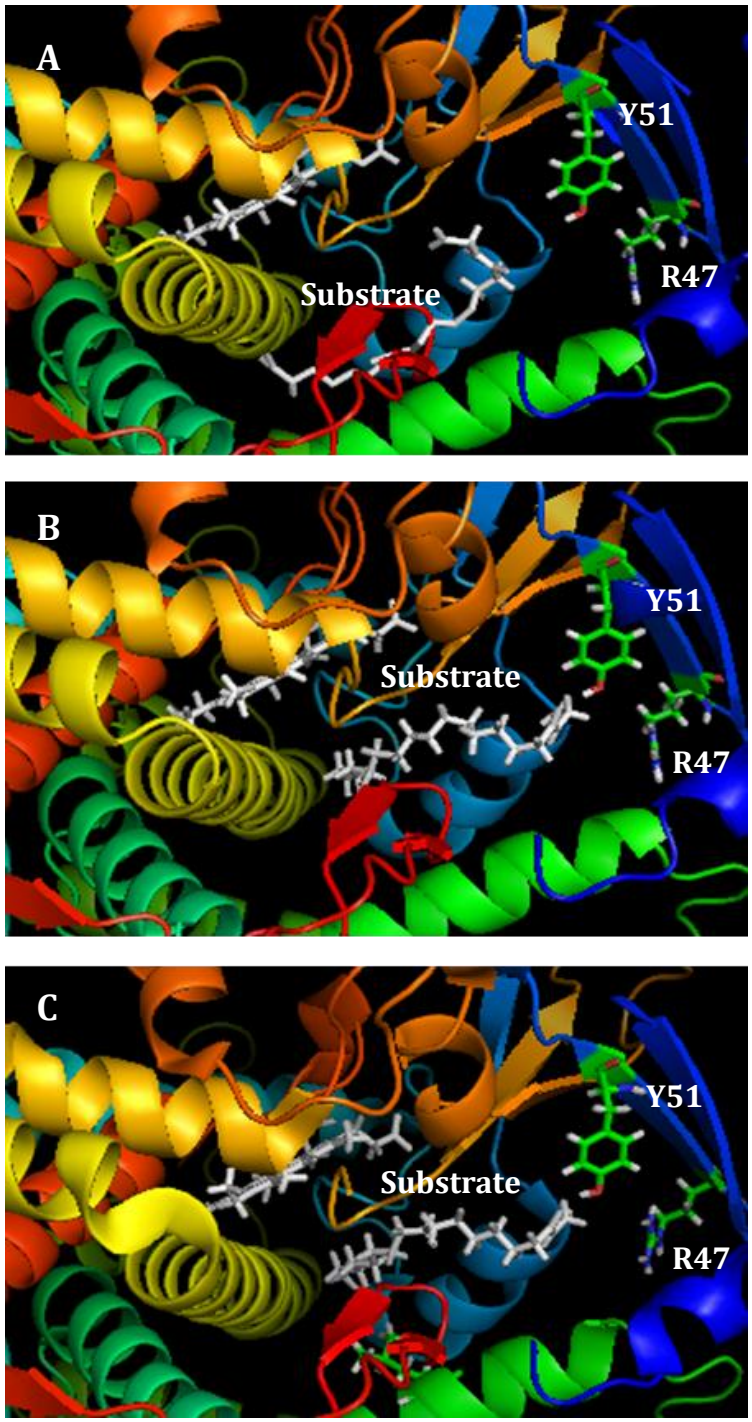

Supplementary Figure 5: Docking of the substrate N-palmitoyl glycine in the binding pocket of P450 hydroxylase. (A) Initial placement of substrate in binding pocket for ligand docking application of ROSETTA. (B) Binding conformation predicted using

ROSETTA. The structure was selected from 1400 models generated. (C) Experimental crystal structure of enzyme-substrate complex obtained through crystallographic data.

The R47/Y51 dyad is known to stabilize the carboxyl group of the substrate through hydrogen bonding [79]. The rationale presented in literature for the L181K mutation was to introduce a R47-like binding interaction. The structure of L181K mutant-complex predicted using ROSETTA suggests that it might not be the case. It can be seen from Supplementary Figure 6 that K181 residue is in fact directed away from the carboxyl group. However, presence of this larger residue (K) makes it favorable for the substrate to achieve a conformation that brings it closer to the heme group, and carboxyl group appears to be stabilized by another residue. These results show the importance of computation to aid the experimental design.

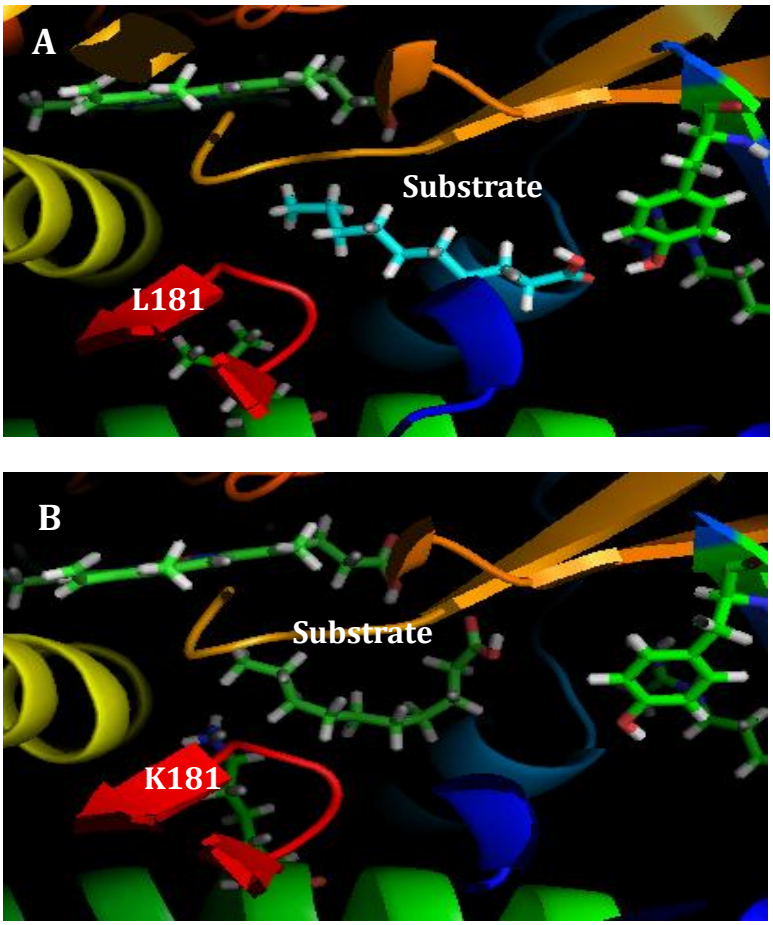

Supplementary Figure 6: Docking of the substrate decanoic acid (DKA) in the binding pocket of P450. (A) Predicted structure for L181K mutant of P450. (B) Predicted structure for wild-type P450.

Bradford assay for P450

The assay was performed as discussed in the materials and methods section. The standard curve was generated using various dilutions of BSA as standard. The standard curve (fir to a straight line) was used to determine concentrations in the unknown cell extract samples. The cell extract concentrations were adjusted so that the absorbance was in the linear range of the standard curve (corresponding to 0.25 to 1 mg/mL of BSA).

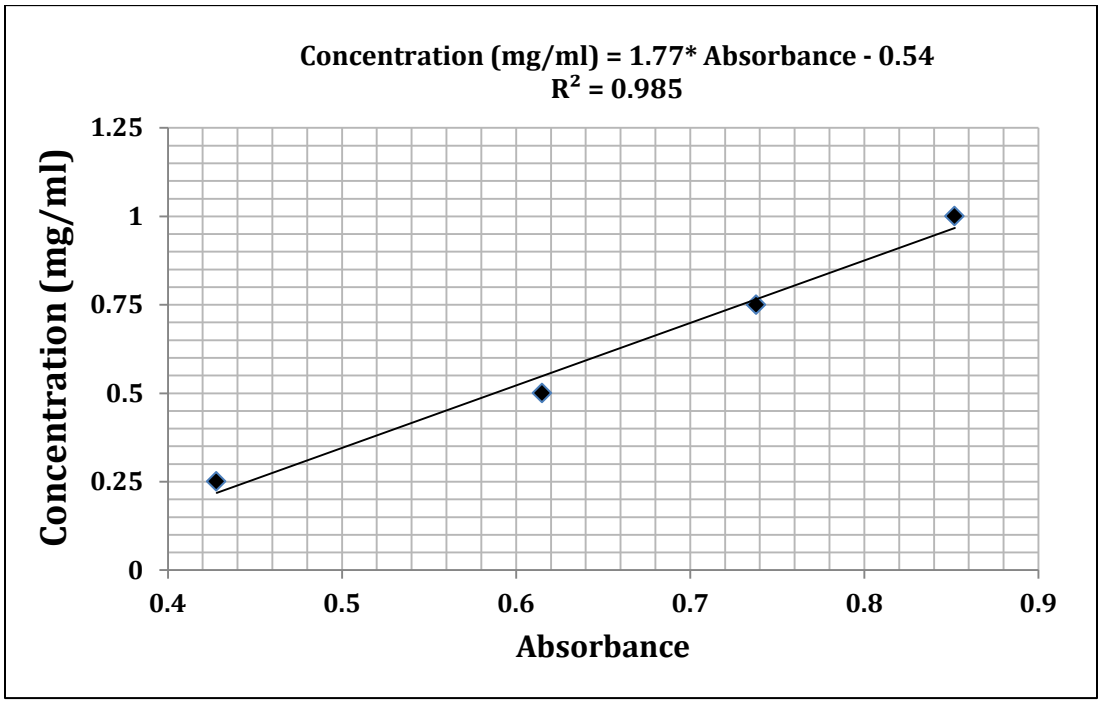

Supplementary Figure 7: The standard curve created using BSA. The data were fit to a straight line, equation of which is also included in the figure.

Supplementary Table 1: Cell extract concentrations determined using Bradford assay

Sample	Concentration in cell extracts (mg/mL)
A74S	0.26
A74H	0.17
A74K	0.19
A328S	0.13
A328H	0.55
A328K	0.21
L437S	0.61
L437H	0.53
L437K	0.71
WT	0.40
L181K	0.58
BL21	0.31
A74S L181K	0.34
L181K L437K	0.44

UV-VIS spectrum of purified P450

Cytochrome P450s are heme-containing proteins. They were discovered as CO-binding pigments in isolated mammalian liver microsomes [88, 89]. In the unbound state, P450 has absorbance peak at 420 nm corresponding to a low spin of ferric-heme compound [90, 91]. When bound to a substrate, the peak shifts to 394 nm, which corresponds to its high spin.

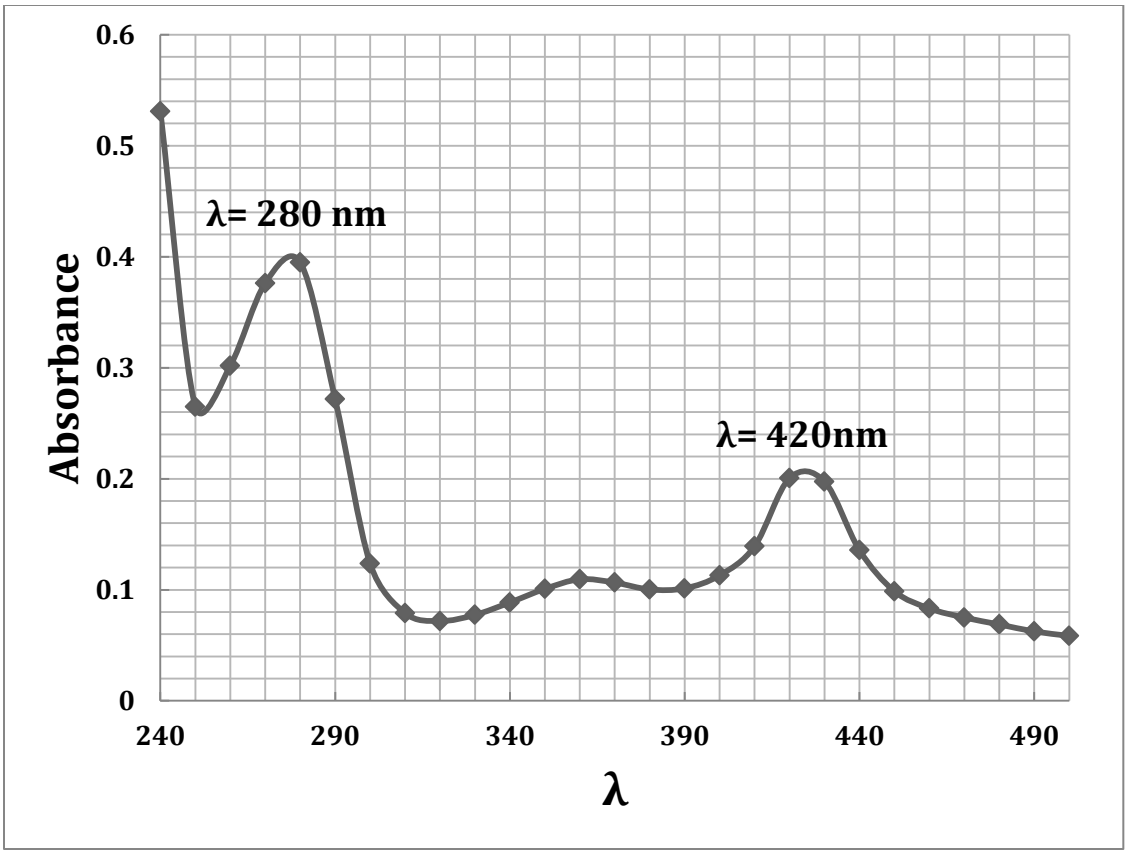

Supplementary Figure 8: UV-VIS spectrum for the purified wild-type P450. The peak at 280 nm is indicative of protein, while the peak at 420 nm is characteristic of P450 enzyme.

Kinetic assay with purified enzymes

The L181K and L437K mutants, along with the wild-type P450 were purified as described in the methods section (Chapter 5). The assay contained 1.25 μM P450 enzyme, 0.625 μM NADPH, 100 mM phosphate buffer (pH=8), and 0 to 250 mM substrate (3-methylbutyric acid) in a total volume of 80 μL. The results are shown in Supplementary Figure 9. It is can be seen that the activities are consistent with the cell extract assays (Figure 11) in that L437K has higher activity than L181K.

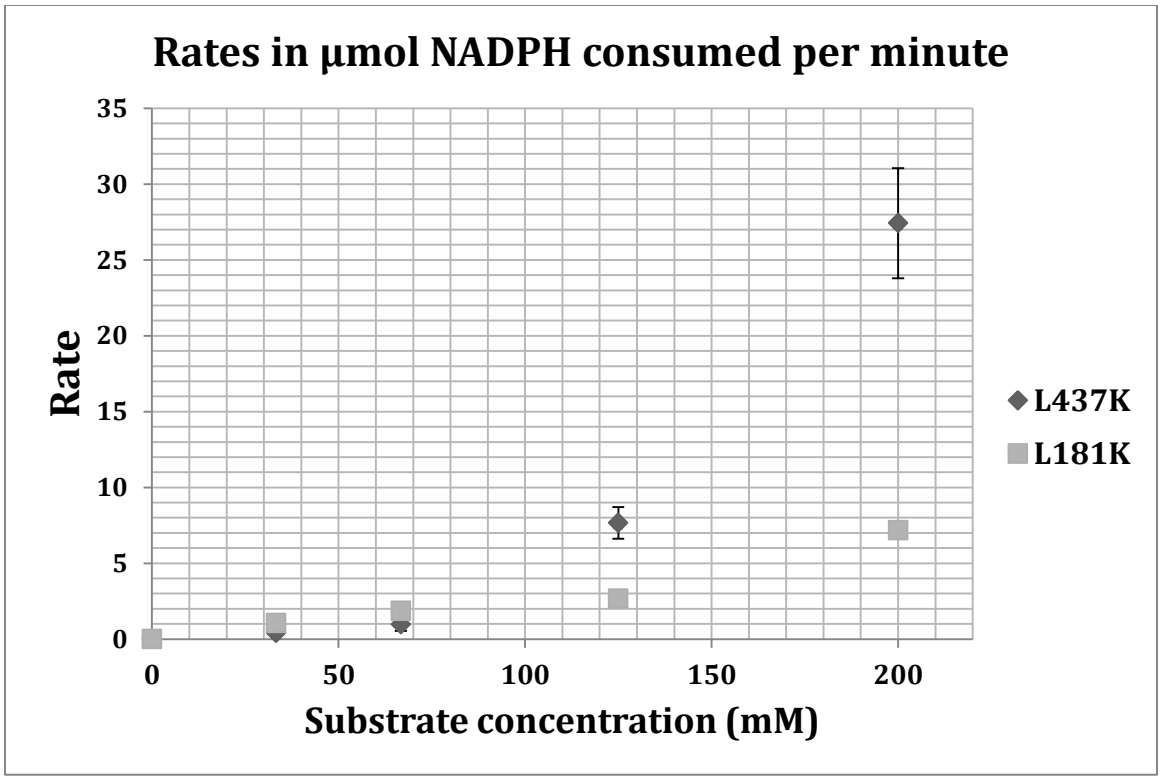

Supplementary Figure 9: Results of the kinetic assay with purified P450 mutants on 3-methylbutyrate. Error bars indicate the standard error (n=3).

References

[1] Ragauskas AJ, Williams CK, Davison BH, Britovsek G, Cairney J, Eckert CA, Frederick WJ, Hallett JP, Leak DJ, Liotta CL. The path forward for biofuels and biomaterials. Science 2006;311:484-489.

[2] MCMAHON T. Historical crude oil prices (table). InflationDatacom vol. 2013; 2013, April 16.

[3] Perlack RD, Wright LL, Turhollow AF, Graham RL, Stokes BJ, Erbach DC. Biomass as feedstock for a bioenergy and bioproducts industry: the technical feasibility of a billion-ton annual supply: DTIC Document; 2005.

[4] Mosier N, Wyman C, Dale B, Elander R, Lee Y, Holtzapple M, Ladisch M. Features of promising technologies for pretreatment of lignocellulosic biomass. Bioresource Technol 2005;96:673-686.

[5] Aida TM, Sato Y, Watanabe M, Tajima K, Nonaka T, Hattori H, Arai K. Dehydration of D-glucose in high temperature water at pressures up to 80 MPa. J Supercrit Fluid 2007;40:381-388.

[6] Ragauskas AJ. The path forward for biofuels and biomaterials. Science 2006;311:484-489.

[7] Chang MCY. Harnessing energy from plant biomass. Curr Opin Chem Biol 2007;11:677-684.

[8] Peralta-Yahya PP, Keasling JD. Advanced biofuel production in microbes. Biotechnol J 2010;5:147-162.

[9] Lynd LR, Laser MS, Bransby D, Dale BE, Davison B, Hamilton R, Himmel M, Keller M, McMillan JD, Sheehan J, Wyman CE. How biotech can transform biofuels. Nat Biotechnol 2008;26:169-172.

[10] Stephanopoulos G. Challenges in engineering microbes for biofuels production. Science 2007;315:801-804.

[11] Baneyx F. Recombinant protein expression in Escherichia coli. Curr Opin Biotechnol 1999;10:411-421.

[12] Zhang FZ, Rodriguez S, Keasling JD. Metabolic engineering of microbial pathways for advanced biofuels production. Curr Opin Biotechnol 2011;22:775-783.

[13] Shendure J, Ji H. Next-generation DNA sequencing. Nat Biotechnol 2008;26:1135-1145.

[14] Bershtein S, Tawfik DS. Advances in laboratory evolution of enzymes. Curr Opin Chem Biol 2008;12:151-158.

[15] Bornscheuer UT, Pohl M. Improved biocatalysts by directed evolution and rational protein design. Curr Opin Chem Biol 2001;5:137-143.

[16] Jonathan R M. Ethanol production from biomass: technology and commercialization status. Curr Opin Microbiol 2001;4:324-329.

[17] Singh SK, Ahmed SU, Pandey A. Metabolic engineering approaches for lactic acid production. Process Biochem 2006;41:991-1000.

[18] Berovic M, Legisa M. Citric acid production. Biotechnol Ann Rev 2007;13:303-343.

[19] González-Pajuelo M, Meynial-Salles I, Mendes F, Andrade JC, Vasconcelos I, Soucaille P. Metabolic engineering of Clostridium acetobutylicum for the industrial production of 1,3-propanediol from glycerol. Metab Eng 2005;7:329-336.

[20] Atsumi S, Wu T-Y, Eckl E-M, Hawkins SD, Buelter T, Liao JC. Engineering the isobutanol biosynthetic pathway in Escherichia coli by comparison of three aldehyde reductase/alcohol dehydrogenase genes. Appl Microbiol Biotechnol 2009;85:651-657.

[21] Zhang K, Li H, Cho KM, Liao JC. Expanding metabolism for total biosynthesis of the nonnatural amino acid L-homoalanine. Proc Natl Acad Sci USA 2010;107:6234-6239.

[22] Yim H, Haselbeck R, Niu W, Pujol-Baxley C, Burgard A, Boldt J, Khandurina J, Trawick JD, Osterhout RE, Stephen R, Estadilla J, Teisan S, Schreyer HB, Andrae S, Yang TH, Lee SY, Burk MJ, Van Dien S. Metabolic engineering of Escherichia coli for direct production of 1,4-butanediol. Nat Chem Biol 2011;7:445-452.

[23] McWhirter C, Lund EA, Tanifum EA, Feng G, Sheikh QI, Hengge AC, Williams NH. Mechanistic study of protein phosphatase-1 (PP1), a catalytically promiscuous enzyme. J Am Chem Soc 2008;130:13673-13682.

[24] Khersonsky O, Roodveldt C, Tawfik DS. Enzyme promiscuity: evolutionary and mechanistic aspects. Curr Opin Chem Biol 2006;10:498-508.

[25] Ljungdhal LG. The autotrophic pathway of acetate synthesis in acetogenic bacteria. Annu Rev Microbiol 1986;40:415-450.

[26] Goswami V, Srivastava AK. Fed-batch propionic acid production by Propionibacterium acidipropionici. Biochem Eng J 2000;4:121-128.

[27] Zigová J, Šturdík E. Advances in biotechnological production of butyric acid. J Ind Microbiol Biotechnol 2000;24:153-160.

[28] Kenealy WR, Cao Y, Weimer PJ. Production of caproic acid by cocultures of ruminal cellulolytic bacteria and Clostridium kluyveri grown on cellulose and ethanol. Appl Microbiol Biotechnol 1995;44:507-513.

[29] Steinbusch KJJ, Hamelers HVM, Plugge CM, Buisman CJN. Biological formation of caproate and caprylate from acetate: fuel and chemical production from low grade biomass. Energy Environ Sci 2011;4:216-224.

[30] Jeon B, Kim B-C, Um Y, Sang B-I. Production of hexanoic acid from d-galactitol by a newly isolated Clostridium sp. BS-1. Appl Microbiol Biotechnol 2010;88:1161-1167.

[31] Dow. Product safety assessment: isopentanoic acid. The Dow chemical company 2008.

[32] Lange J-P, Price R, Ayoub PM, Louis J, Petrus L, Clarke L, Gosselink H. Valeric biofuels: a platform of cellulosic transportation fuels. Angew Chem Int Edit 2010;49:4479-4483.

[33] Bueding E, Yale HW. Production of α-methylbutyric acid by bacteria-free Ascaris lumbricoides. J Biol Chem 1951;193:411-423.

[34] Saz HJ, Weil A. The mechanism of the formation of α-methylbutyrate from carbohydrate by Ascaris lumbricoides muscle. J Biol Chem 1960;235:914-918.

[35] Satter LD, Esdale WJ. In vitro lactate metabolism by ruminal ingesta. Appl Microbiol 1968;16:680-688.

[36] Russell JB, Martin SA. Effects of various methane inhibitors on the fermentation of amino acids by mixed rumen microorganisms in vitro. J Anim Sci 1984;59:1329-1338.

[37] Fang HHP, Liu H. Effect of pH on hydrogen production from glucose by a mixed culture. Bioresource Technol 2002;82:87-93.

[38] Atsumi S, Hanai T, Liao JC. Non-fermentative pathways for synthesis of branched-chain higher alcohols as biofuels. Nature 2008;451:86-89.

[39] Zhang KC, Sawaya MR, Eisenberg DS, Liao JC. Expanding metabolism for biosynthesis of nonnatural alcohols. Proc Natl Acad Sci USA 2008;105:20653-20658.

[40] Zhang K, Woodruff AP, Xiong M, Zhou J, Dhande YK. A synthetic metabolic pathway for production of the platform chemical isobutyric acid. ChemSusChem 2011;4:1068-1070.

[41] Xiong M, Deng J, Woodruff AP, Zhu M, Zhou J, Park SW, Li H, Fu Y, Zhang K. A bio-catalytic approach to aliphatic ketones. Sci Rep 2012;2.

[42] Ditre CM, Griffin TD, Murphy GF, Sueki H, Telegan B, Johnson WC, Yu RJ, Van Scott EJ. Effects of alpha-hydroxy acids on photoaged skin: a pilot clinical, histologic, and ultrastructural study. J Am Acad Dermatol 1996;34:187.

[43] Li SM, Garreau H, Vert M. Structure-property relationships in the case of the degradation of massive aliphatic poly-(α-hydroxy acids) in aqueous media. J Mater Sci- Mater M 1990;1:123-130.

[44] Vert M, Li S, Spenlehauer G, Guerin P. Bioresorbability and biocompatibility of aliphatic polyesters. J Mater Sci- Mater M 1992;3:432-446.

[45] Gierl A. The cytochrome P450 superfamily of monooxygenases. Handb Maize: Springer; 2009. p. 731-739.

[46] Nelson DR, Koymans L, Kamataki T, Stegeman JJ, Feyereisen R, Waxman DJ, Waterman MR, Gotoh O, Coon MJ, Estabrook RW. P450 superfamily: update on new sequences, gene mapping, accession numbers and nomenclature. Pharmacogenet Genom 1996;6:1-42.

[47] Narhi LO, Fulco AJ. Characterization of a catalytically self-sufficient 119,000-dalton cytochrome P-450 monooxygenase induced by barbiturates in Bacillus megaterium. J Biol Chem 1986;261:7160-7169.

[48] Kumar S. Engineering cytochrome P450 biocatalysts for biotechnology, medicine and bioremediation. Expert Opin Drug Met 2010;6:115-131.

[49] Bernhardt R. Cytochromes P450 as versatile biocatalysts. J Biotechnol 2006;124:128-145.

[50] Sakaki T. Practical application of cytochrome p450. Biol Pharm Bull 2012;35:844-849.

[51] Munro AW, Leys DG, McLean KJ, Marshall KR, Ost TW, Daff S, Miles CS, Chapman SK, Lysek DA, Moser CC. P450 BM3: the very model of a modern flavocytochrome. Trends Biochem Sci 2002;27:250-257.

[52] Warman A, Roitel O, Neeli R, Girvan H, Seward H, Murray S, McLean K, Joyce M, Toogood H, Holt R. Flavocytochrome P450 BM3: an update on structure and mechanism of a biotechnologically important enzyme. Biochem Soc T 2005;33:747-753.

[53] Ost TW, Clark J, Mowat CG, Miles CS, Walkinshaw MD, Reid GA, Chapman SK, Daff S. Oxygen activation and electron transfer in flavocytochrome P450 BM3. J Am Chem Soc 2003;125:15010-15020.

[54] Farinas ET, Schwaneberg U, Glieder A, Arnold FH. Directed evolution of a cytochrome P450 monooxygenase for alkane oxidation. Adv Synth Catal 2001;343:601-606.

[55] Fasan R, Meharenna YT, Snow CD, Poulos TL, Arnold FH. Evolutionary history of a specialized P450 propane monooxygenase. J Mol Biol 2008;383:1069-1080.

[56] Fasan R, Chen MM, Crook NC, Arnold FH. Engineered alkane-hydroxylating cytochrome P450BM3 exhibiting nativelike catalytic properties. Angew Chem 2007;119:8566-8570.

[57] Li Q-S, Ogawa J, Schmid RD, Shimizu S. Engineering cytochrome P450 BM-3 for oxidation of polycyclic aromatic hydrocarbons. Appl Environ Microbiol 2001;67:5735-5739.

[58] Alcalde M, Farinas ET, Arnold FH. Colorimetric high-throughput assay for alkene epoxidation catalyzed by cytochrome P450 BM-3 variant 139-3. J Biomol Screen 2004;9:141-146.

[59] Ost TW, Miles CS, Murdoch J, Cheung Y-F, Reid GA, Chapman SK, Munro AW. Rational re-design of the substrate binding site of flavocytochrome P450 BM3. FEBS letters 2000;486:173-177.

[60] Boddupalli SS, Pramanik BC, Slaughter CA, Estabrook RW, Peterson JA. Fatty acid monooxygenation by P450 BM-3: Product identification and proposed mechanisms for the sequential hydroxylation reactions. Arch Biochem Biophys 1992;292:20-28.

[61] Huang W-D, Zhang Y-HP. Analysis of biofuels production from sugar based on three criteria: thermodynamics, bioenergetics, and product separation. Energy Environ Sci 2011;4:784-792.

[62] Presser KA, Ratkowsky DA, Ross T. Modeling the growth rate of Escherichia coli as a function of pH and lactic acid concentration. Appl Environ Microbiol 1997;63:2355-2360.

[63] Keshavarz T, Roy I. Polyhydroxyalkanoates: bioplastics with a green agenda. Curr Opin Microbiol 2010;13:321-326.

[64] Suriyamongkol P, Weselake R, Narine S, Moloney M, Shah S. Biotechnological approaches for the production of polyhydroxyalkanoates in microorganisms and plants—a review. Biotechnol Adv 2007;25:148-175.

[65] Marcheschi RJ, Li H, Zhang K, Noey EL, Kim S, Chaubey A, Houk K, Liao JC. A synthetic recursive "+ 1" pathway for carbon chain elongation. ACS Chem Biol 2012;7:689-697.

[66] de la Plaza M, Fernandez de Palencia P, Pelaez C, Requena T. Biochemical and molecular characterization of alpha-ketoisovalerate decarboxylase, an enzyme involved in the formation of aldehydes from amino acids by Lactococcus lactis. FEMS Microbiol Lett 2004;238:367-374.

[67] Rodríguez-Zavala JS, Allali-Hassani A, Weiner H. Characterization of E. coli tetrameric aldehyde dehydrogenases with atypical properties compared to other aldehyde dehydrogenases. Protein Sci 2006;15:1387-1396.

[68] Ho KK, Weiner H. Isolation and characterization of an aldehyde dehydrogenase encoded by the aldB Gene of Escherichia coli. J Bacteriol 2005;187:1067-1073.

[69] Jo J-E, Mohan Raj S, Rathnasingh C, Selvakumar E, Jung W-C, Park S. Cloning, expression, and characterization of an aldehyde dehydrogenase from Escherichia coli K-12 that utilizes 3-Hydroxypropionaldehyde as a substrate. Appl Microbiol Biotechnol 2008;81:51-60.

[70] Bartsch K, von Johnn-Marteville A, Schulz A. Molecular analysis of two genes of the Escherichia coli gab cluster: nucleotide sequence of the glutamate:succinic semialdehyde transaminase gene (gabT) and characterization of the succinic semialdehyde dehydrogenase gene (gabD). J Bacteriol 1990;172:7035-7042.

[71] Gruez A, Roig-Zamboni V, Grisel S, Salomoni A, Valencia C, Campanacci V, Tegoni M, Cambillau C. Crystal structure and kinetics identify Escherichia coli YdcW gene product as a medium-chain aldehyde dehydrogenase. J Mol Biol 2004;343:29-41.

[72] Watanabe S, Yamada M, Ohtsu I, Makino K. α-Ketoglutaric semialdehyde dehydrogenase isozymes involved in metabolic pathways of D-glucarate, D-galactarate, and hydroxy-L-proline: molecular and metabolic convergent evolution. J Biol Chem 2006;282:6685-6695.

[73] McClelland M, Wilson RK. Comparison of sample sequences of the Salmonella typhi genome to the sequence of the complete Escherichia coli K-12 genome. Infect Immun 1998;66:4305-4312.

[74] Valgepea K, Adamberg K, Nahku R, Lahtvee P-J, Arike L, Vilu R. Systems biology approach reveals that overflow metabolism of acetate in Escherichia coli is triggered by carbon catabolite repression of acetyl-CoA synthetase. BMC Syst Biol 2010;4:166.

[75] Vemuri GN, Altman E, Sangurdekar DP, Khodursky AB, Eiteman MA. Overflow Metabolism in Escherichia coli during Steady-State Growth: Transcriptional Regulation and Effect of the Redox Ratio. Appl Environ Microbiol 2006;72:3653-3661.

[76] Campbell JW, Morgan-Kiss RM, E. Cronan J. A new Escherichia coli metabolic competency: growth on fatty acids by a novel anaerobic β-oxidation pathway. Mol Microbiol 2003;47:793-805.

[77] Kaufmann KW, Lemmon GH, DeLuca SL, Sheehan JH, Meiler J. Practically useful: what the Rosetta protein modeling suite can do for you. Biochemistry 2010;49:2987-2998.

[78] Leaver-Fay A, Tyka M, Lewis SM, Lange OF, Thompson J, Jacak R, Kaufman K, Renfrew PD, Smith CA, Sheffler W. ROSETTA3: an object-oriented software suite for the simulation and design of macromolecules. Methods Enzymol 2011;487:545-574.

[79] Cowart LA, Falck JR, Capdevila JH. Structural determinants of active site binding affinity and metabolism by cytochrome P450 BM-3. Arch Biochem Biophys 2001;387:117-124.

[80] Bloom JD, Labthavikul ST, Otey CR, Arnold FH. Protein stability promotes evolvability. Proc Natl Acad Sci USA 2006;103:5869-5874.

[81] Haines DC, Hegde A, Chen B, Zhao W, Bondlela M, Humphreys JM, Mullin DA, Tomchick DR, Machius M, Peterson JA. A single active-site mutation of P450BM-3 dramatically enhances substrate binding and rate of product formation. Biochemistry 2011;50:8333-8341.

[82] Sokatch JR, Sanders LE, Marshall VP. Oxidation of methylmalonate semialdehyde to propionyl coenzyme A in Pseudomonas aeruginosa grown on valine. J Biol Chem 1968;243:2500-2506.

[83] Brock M, Maerker C, Schütz A, Völker U, Buckel W. Oxidation of propionate to pyruvate in Escherichia coli. Eur J Biochem 2002;269:6184-6194.

[84] William W K. Genetic control of the metabolism of propionate by Escherichia coli K12. Biochim Biophys Acta 1972;264:508-521.

[85] Bannerjee D, Sanders LE, Sokatch JR. Properties of aurified methylmalonate semialdehyde dehydrogenase of Pseudomonas aeruginosa. J Biol Chem 1970;245:1828-1835.

[86] Steele MI, Lorenz D, Hatter K, Park A, Sokatch JR. Characterization of the mmsAB operon of Pseudomonas aeruginosa PAO encoding methylmalonate-semialdehyde dehydrogenase and 3-hydroxyisobutyrate dehydrogenase. J Biol Chem 1992;267:13585-13592.

[87] Baba T, Ara T, Hasegawa M, Takai Y, Okumura Y, Baba M, Datsenko KA, Tomita M, Wanner BL, Mori H. Construction of Escherichia coli K-12 in-frame, single-gene knockout mutants: the Keio collection. Mol Syst Biol 2006;2:2006.0008.

[88] Klingenberg M. Pigments of rat liver microsomes. Arch Biochem Biophys 1958;75:376-386.

[89] Garfinkel D. Studies on pig liver microsomes. I. Enzymic and pigment composition of different microsomal fractions. Arch Biochem Biophys 1958;77:493-509.

[90] Tsai R, Yu C, Gunsalus I, Peisach J, Blumberg W, Orme-Johnson W, Beinert H. Spin-state changes in cytochrome P-450cam on binding of specific substrates. Proc Natl Acad Sci USA 1970;66:1157-1163.

[91] Miles J, Munro A, Rospendowski B, Smith W, McKnight J, Thomson A. Domains of the catalytically self-sufficient cytochrome P-450 BM-3. Genetic construction, overexpression, purification and spectroscopic characterization. Biochem J 1992;288:503.